COMPARITIVE STUDY OF FLOW FIELD AROUND CIRCULAR UNIFORM PIER IN SCOUR HOLE WITH THAT AROUND THE CIRCULAR UNIFORM PIER PLACED IN RIGID BED

Project Report submitted in partial fulfillment of the requirement for the degree of

Master of Technology

In

Structural Engineering

Under the Supervision of

Dr. Ashish Kumar

By

Hari Krishan Pandit

(132660)

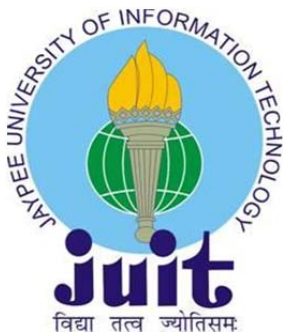

Department of Civil Engineering

Jaypee University of Information and Technology
Waknaghat, Solan – 173234, Himachal Pradesh 2015

CERTIFICATE

This is to certify that the work which is being presented in the project title **"COMPARITIVE STUDY OF FLOW FIELD AROUND CIRCULAR UNIFORM PIER WITH THAT AROUND THE CIRCULAR UNIFORM PIER PLACED IN RIGID BED"** in partial fulfillment of the requirements for the award of the degree of Master of technology and submitted in Civil Engineering Department, Jaypee University of Information Technology, Waknaghat is an authentic record of work carried out by **Hari Krishan Pandit** during a period from August 2014 to May 2015 under the supervision of **Dr. Ashish Kumar** Associate Professor, Civil Engineering Department, Jaypee University of Information Technology, Waknaghat.

The above statement made is correct to the best of my knowledge.

Date: - ……

Prof. Dr. Ashok Kumar Gupta	Dr. Ashish Kumar	……
Professor & Head of Department	Associate Professor	External Examiner
Civil Engineering Department	Civil Engineering Department	
JUIT Waknaghat	JUIT Waknaghat	

DECLARATION

I hereby declare that the research work presented in this Project entitled "*COMPARITIVE STUDY OF FLOW FIELD AROUND CIRCULAR UNIFORM PIER WITH THAT AROUND THE CIRCULAR UNIFORM PIER PLACED IN RIGID BED"* submitted for the award of the degree of Master of technology in the Department of Civil Engineering, Jaypee University of Information and Technology Wakhnaghat, is original and my own account of research. This research work is independent and its main content work has not previously been submitted for degree at any university in India or Abroad.

(Hari Krishan Pandit)

ACKNOWLEDGEMENT

I wish to express my sincere gratitude to **Dr. Ashish Kumar,** for his excellent guidance and perennial encouragement and support during the course of my work in the last one year. I truly appreciate and value his profound knowledge, esteemed supervision and encouragement from the beginning to the end of this thesis.

My special thanks are due to **Prof. Ashok Gupta,** Head of the Civil Engineering Department, for all the facilities provided to successfully complete this work.

I am also very thankful to all the faculty members of the department, especially Structural Engineering specialization for their constant encouragement during the project.

I also take the opportunity to thank all my friends who have directly or indirectly helped me in my project work and in the completion of this report.

Last but not the least I would like to thank my parents, who taught me the value of hard work by their own example. I would like to share this bite of happiness with my mother and father. They rendered me enormous support during the whole tenure of my stay at JUIT, Waknaghat

.

.

Date: **Hari Krishan Pandit**

ABSTRACT

In the present study experiments were carried out to measure the flow structure and turbulence characteristics around uniform circular pier in the absence and as well as in the presence of scour hole under clear water condition. The pier comprised of pier diameter = 115 mm. Two experimental runs were conducted in which an Acoustic Doppler Velocimeter (ADV) was used to measure the instantaneous velocity components, turbulent intensity components and Reynolds' stresses at the central line of pier in the upstream plane. A comparative study between these flow structures is therefore presented herein. The flow characteristics around the circular uniform pier in scour hole are moreover same as compared to the flow characteristics around the circular uniform pier without scour hole. The horseshoe vortex can be considered as the basic mechanism causing scour around the bridge piers.

Index

LIST OF FIGURES

LIST OF TABLES

LIST OF SYMBOLS AND ABBREVIATIONS

Symbols

A_0	= cross-sectional area of primary vortex
A_s	= cross-sectional area of scour hole at time t
A_t	= cross-sectional area of the principal vortex
b	= diameter or width of bridge pier
B	= flume width
d	= size of uniform sediment
d_{50}	= median sediment grain diameter
d_{st}	= depth of scour below the initial bed level at time t
D_*	= dimensionless sediment size
F_r	= Froude number $U_\infty/(gh)^{0.5}$
g	= gravitational acceleration
h	= depth of flow
k	= turbulent kinetic energy
L_p	= length of pier
Q	= discharge
r	= distance in radial direction
r_p	= radius of pier
R_{eb}	= pier Reynolds number
S	= energy slope
u, v, w	= Cartesian velocity components in x, y and z directions respectively
u', v', w'	= fluctuation of u, v, and w components of velocity respectively
u_*	= bed shear velocity of approach flow
u_{*c}	= critical bed shear velocity for d_{50} size, defined by Shields' function
u_{*t}	= shear velocity at time t
U_∞	= velocity of approach flow
U_c	= velocity of approach flow corresponding to incipient motion of sediment

particle in approach flow

z = distance in vertical direction in Cartesian and cylindrical coordinates system

Z = height of the top of the foundation above the initial bed level = -Y

σ_g = geometric standard deviation of the sediment

ϕ = angle of repose of sediment

γ_f = specific weight of fluid

γ_s = specific weight of sediment

$\Delta\gamma_s$ = $\gamma_s - \gamma_f$

$\sqrt{\overline{u'u'}}$, $\sqrt{\overline{v'v'}}$ = longitudinal and transverse components of turbulence intensity

$\sqrt{\overline{w'w'}}$ = vertical component of turbulence intensity

$\overline{u'w'}$, $\overline{v'w'}$ = components of Reynolds' Stress

Abbreviations

UPSH experimental run in which scour hole was allowed to develop around the circular uniform pier (b = 115 mm)

UPRB experimental run in which circular uniform pier (b = 115 mm) was placed on the rigid bed

Chapter 1
INTRODUCTION

1.1 GENERAL

Bridges are required in order to cross the waterways by transport carriers. Thus bridges provide a smooth way to the transportation system. Piers, upon which the superstructure of the bridge rest play an important role in bridge stability and safety. A main cause of bridge failure is scour by the flow around its piers and abutments (Melville and Coleman, 2000). Thus one of the main concerns about the stability of bridge foundation is the correct estimation of local scour depth around the bridge piers. The process of scour around bridge pier involves the complexities of both the three-dimensional flow patterns and the sediment transport. The scour process around the pier is a result of the development of high shear stress due to the three-dimensional separation of the boundary layer on the pier upstream which results in a high level of turbulence and vorticity around the piers (Garde and Ranga Raju, 2000). Figure 1.1 shows the principal components of flow structure at a circular bridge pier. These elements (details discussed subsequently) of flow individually or in combination, result in local scour around the pier. A combination of the strong down flow and the horseshoe vortex are considered by many to be the prime agents causing significant scour around the bridge elements like piers and abutments.

The accurate estimation of scour extent and its depth at bridge sites is a major concern for the hydraulic engineers. The underestimation of scour depth results in designing too shallow foundation and thus providing a chance of exposure of the

foundation to the flow which is dangerous for the safety of the bridge whereas overestimation of the scour depth results in uneconomical design.

1.2 PRESENT STATE OF KNOWLEDGE ON BRIDGE SCOUR

A large number of investigations have been carried out over past five decades, mostly focused on the development of the relationships for computation of equilibrium or maximum scour depth around the circular uniform bridge piers. But actual bridge piers are non- uniform in cross-sections along their heights. Only a few studies have been conducted on the estimation of scour depth around compound bridge piers. A brief review on scour around uniform bridge piers. Detailed review however, is presented in the Chapter 2.

1.2.1 Scour around Uniform Bridge Pier

The phenomenon of scour around bridge piers has been studied extensively by a large number of investigators. Numerous studies have been conducted to develop the relationships for scour depth estimation at uniform shaped piers. In India the design depth of scour at bridge piers is estimated as per procedure given in IRC: 78, (2000) and IRC: 5, (1998). Other methods for estimation of scour depth include those by Laursen and Toch, (1956); Shen *et al*., (1969); Breusers *et al*., (1977); Jain and Fisher, (1979); Melville and Sutherland, (1988); Kothyari *et al*., (1992 a, b); Melville, (1997); Cardoso and Bettess, (1999); Melville and Coleman, (2000); HEC-18, (Richardson and Davis, 2001) and Sheppard *et al*., (2004) *etc*.

Several researchers have also studied the effect of sediment non-uniformity on scour (Ettema, 1980; Kothyari, 1989; Oliveto and Hager, 2002; Chang *et al*., 2004). The temporal variation of scour depth is also studied in detail (Chabert and Engeldinger, 1956; Ettema, 1980; Yanmaz and Altinbilek, 1991; Kothyari *et al*., 1992 a, b; Melville and Chiew, 1999; Oliveto and Hagar, 2002, 2005; Mia and Nago, 2003; Chang *et al*., 2004 and Yanmaz, 2006). Effect of flow unsteadiness on bridge pier scour has been studied among others by Kothyari *et al*., (1992 a, b); Chang *et al*., (2004) and Oliveto and Hager, (2005).

1.2.2 Flow Pattern Around Circular Uniform Piers

Relatively large number of investigations has been made on development of scour hole and scour depth estimation, lesser number of studies however, are reported for investigations on flow pattern around the uniform piers with or without the presence of a scour hole. A few such studies have been made however more recently using uniform circular piers by Melville and Raudkivi, (1977); Dey *et al*., (1995); Ahmed and Rajaratnam, (1998); Graf and Istiarto, (2002); Muzzammil and Gangadhariah, (2003); Dey and Raikar, (2007) *etc*. Melville and Raudkivi (1977) were amongst the first to conduct experiments for studying the flow pattern around the circular piers. Experiments were conducted at three stages of scour *viz.* initial flat bed, the intermediate scour hole after 30 minutes from the commencement of erosion and the final equilibrium scour hole. The measurements of flow field and turbulence structure around the pier were made with hot film wire anemometer and pitot tube. From the observations they described that the

horseshoe vortex travels along the perimeter of the pier. Strength of the horseshoe vortex was quantified. Accordingly, Raudkivi (1990) presented Fig. 1.1 showing the various scouring elements of the flow which act individually as well as in combination causing the development of scour around the pier. More recently Dey *et al*. (1995) studied the three-dimensional kinematic field of the vortex around circular piers in a quasi-equilibrium scour condition under a clear water regime. Their study was based on the velocity data obtained from the laboratory experiments conducted by using a 5-yaw and a 3-yaw pitot tubes. On the basis of experimental results Ahmed and Rajaratnam (1998, 2000) described the velocity profiles in the upstream plane of symmetry by the Clauser type defect scheme. They reported that in the presence of scour hole, the upstream flow accelerates into the scour hole rather than separating from the bed. A down flow velocity at the pier upstream portion that could be up to 95 percent of the approach velocity was observed. Graf and Istiarto (2002) carried out detailed flow observations in the plane before and after the pier in the established (equilibrium) scour hole. Results of their study showed that a vortex system is established in front of the pier and a trailing wake vortex system of strong turbulence is formed behind the pier. Muzammil and Gangadhariah (2003) investigated the characteristics of the primary vortex on the plane of symmetry in front of a cylinder during the entire process of scouring and concluded that the vortex velocity and strength shows increasing trends in the initial stage of scour process and a decreasing trend in the last stage of scour process. Dey and Raikar (2007) conducted the experimental study around the circular uniform pier to measure the flow field within the developing and established scour hole. The flow field measurement was taken by Acoustic Doppler Velocimeter (*ADV*). The flow measurements were also taken within the

scour hole around the square pier with side facing the approach flow. On the basis of study they concluded that, within the scour hole, there exist a core of higher magnitude of turbulence intensities and Reynolds' stresses that increases with the development of the scour hole.

1.3 OBJECTIVES

The present study was taken up to fulfill the above mentioned gaps in knowledge on bridge pier scour. The broad objective of the investigation was to conduct a carefully controlled set of experiments for deriving a better understanding of the flow and the turbulence characteristics around the uniform circular pier on the rigid bed and with the scour hole. The information retrieved on the flow structures around the piers is used next to validate and further develop.

The following specific objectives were stipulated for the present study:

(i) To study the flow and the turbulence characteristics around the circular uniform pier founded in the rigid bed as well as in the scour hole.

(ii) To compare flow pattern around uniform circular pier with scour and in rigid bed (without scour) condition.

1.4 LIMITATIONS

The followings are main limitations of the present study:

(ii) The present study is confined to clear-water scour condition. Uniform circular pier having diameter of 115mm was used during the experiments.

(ii) Uniform cohesion less sediment of size 0.55 mm and relative density of 2.58 was used in the laboratory experiments.

(iii) The experiments are restricted to the case of steady uniform flows.

Chapter 2
REVIEW OF LITERATURE

2.1 GENERAL

The process of scour around bridge piers is complex due to three-dimensional flow distribution and sediment transport around the pier. A lot of investigations have been carried out in the past mainly with the objective of developing relationships for maximum scour depth. As a result, a large amount of literature is available on the topic of bridge scour and also on its control. A handful of studies only are however available on the flow field around the bridge piers. Mainly the flow pattern within the scour hole around circular uniform bridge piers has been studied amongst others by Melville and Raudkivi, (1977); Dey *et al.*, (1995); Ahmed and Rajaratnam, (1998); Graf and Istiarto, (2002); Muzzammil and Gangadhariah, (2003) and Dey and Raikar, (2007).

A detailed review of literature available on the afore-mentioned topics is presented in the following sections:

2.2 SCOUR AROUND UNIFORM PIER

The subject of scour at bridge piers of uniform geometry has been extensively investigated and well documented. A few of the many contributors to this literature are Laursen and Toch, (1956); Shen *et al*., (1969); Melville and Sutherland, (1988); Melville, (1997); Melville and Coleman, (2000); Muzzammil and Gangadhariah, (2003) *etc*. The process of scour is affected by several factors like the flow, fluid, pier and bed material characteristics. The scour process around the pier is time dependent. The mechanism

takes place with time. Depending upon whether the upstream flow is transporting sediment or not the pier scour is conventionally classified as

(i) clear-water scour; while the upstream flow is free of sediment and

(ii) live–bed scour; while the upstream flow is transporting sediment. It is commonly believed that the equilibrium scour depth in live-bed conditions is slightly smaller than that in clear-water scour condition (Shen *et al*., 1969).

2.2.1 Equilibrium Scour Depth Around Uniform Pier

Several empirical and semi-analytical studies for the estimation of maximum or equilibrium scour depth around uniform bridge piers are available in literature. A detailed description on pier scour relationships can be found in Melville, (1975); Ettema, (1980); Kothyari, (1989); Kumar, (1996) and Garde and Ranga Raju, (2000). Hence the same is not repeated here.

2.2.2 Flow Pattern Around Circular Uniform Pier

Melville and Raudkivi (1977) were amongst the first to conduct experiments for study of flow pattern around a circular uniform pier during the three stages of scour *viz.* initial flat bed, the intermediate scour hole developed after 30 minutes from its commencement and the final equilibrium scour hole. Experiments were conducted in a 19 m long, 0.456 m wide and 0.44 m deep flume. The sediment having size d_{50} = 0.385 mm was used. The clear-water condition prevailed during the experiments. The measurements of flow field and turbulence structure around the pier were made with hot film wire

anemometer and pitot tube. From the observations they noted the horseshoe vortex to be initially small and approximately circular in cross-section. During the development of scour hole, the shape of vortex was reported to follow the combined shape of pier and scour hole. The vortex expands during scouring and sinks in the scoured area and its centre moves down into the scour hole and simultaneously drifts away from the pier surface. The horseshoe vortex was observed to travel along the perimeter of the pier. Strength of horseshoe vortex during different scour phases was also quantified.

Dey *et al*. (1995) conducted experiments in a 10 m long, 0.81 m wide and 0.25 m deep flume to study the flow field within a quasi- equilibrium scour hole around the circular uniform pier. The experiments were conducted in clear-water regime. The three-dimensional velocity components were measured using a 5-yaw and a 3-yaw pitot tubes. On the basis of observed velocity pattern they developed a three-dimensional semi-empirical kinematic model for vortex flow around circular piers in a quasi-equilibrium scour under clear-water regime. Their model results showed satisfactory agreement with the velocity distribution pattern of Melville's experiments (Melville, 1975).

Ahmed and Rajaratnam (1998) also conducted detailed experiments on the flow past circular uniform piers placed on smooth, rough and mobile beds. The experiments were conducted in a flume 20 m long and 1.22 m wide, with a sediment recess 0.2 m deep, 0.78 m wide and 0.78 m long which was long enough to accommodate the scoured bed around the circular pier. The velocity vectors and bed shear stress vector were measured with two 3-tube yaw probes. The flow was noticed to pass through the scour hole which was reflected by a stronger downflow. The bed roughness was observed to induce a steeper pressure gradient and thus a stronger downflow in front of the pier.

Based on experiments these investigators concluded that in the presence of scour hole, the upstream flow accelerates into the scour hole rather than separating from the bed. They further reported that down flow velocity in front of the pier reached as much as 95 percent of the approach velocity inside the scour hole before diminishing again. From the limited amount of data for rigid bed experiments, they reported that the maximum downflow in the absence of scour hole was about 35% of the approach flow. The velocity profiles in the upstream plane of symmetry were represented by Clauser type defect scheme.

Graf and Istiarto (2002) carried out experiments related to velocity measurements in a established (equilibrium) scour hole around a circular uniform pier of diameter 0.15 m under clear-water scour condition. The experiments were conducted in a 29 m long, 2.45 m wide rectangular channel having uniform sediment bed of mean diameter d_{50} = 2.1 mm. An Acoustic Doppler Velocity Profiler (*ADVP*) was used to simultaneously measure the instantaneous values of the three components of velocity in the plane before and after the pier within the scour hole. Throughout the measurements the bed shear stress was noticed to be smaller than the Shields' critical value. The distributions of the turbulence intensity as well as of the Reynolds' stress were evaluated. The turbulent kinetic energy was observed to be very strong at the foot of the pier on the upstream side. It was also reported to be very strong in the wake behind the pier.

Following conclusions were drawn from their study.

(a) A vortex system is established in front of the pier and a trailing wake vortex system of strong turbulence is formed behind the pier.

(b) In the downstream reach of the pier there exist a flow reversal towards the water surface. This is rather pronounced immediately after the pier, but gradually returns to a logarithmic profile further downstream. The vorticity in this region is rather weak.

(c) The bed shear stress is considerably reduced in the scour hole upstream of the pier when compared to its value in the approach flow.

Muzammil and Gangadhariah (2003) experimentally investigated the dynamics of scour hole development around the circular uniform pier. The experiments were conducted in a glass walled flume of length 5.0 m and width 0.5 m with sediment of median size 0.16 mm and 0.6 mm. Circular hollow glass cylinders were used as piers with diameters varying from 31.0 mm to 78.5 mm. The mudflow visualization technique developed by them was used to visualize the horseshoe vortex in the plane of symmetry in front of pier. They characterized the horseshoe vortex in terms of vortex dimensions, tangential velocity and strength for flows as rigid bed, on solidified scour bed and on mobile sediment bed. They also developed an expression for estimation of equilibrium scour depth based on the vortex velocity variation in scour hole and validated it by using some experimental data. They concluded that:

(a) In the rigid bed, the mean size of the primary vortex of the horseshoe vortex system is about 20% of the pier diameter in size, while the vortex tangential velocity is approximately 50% of the mean velocity of the approach flow for $10^4 \leq Re_b \leq 1.4 \times 10^5$, here Re_b is the pier Reynolds number.

(b) As the scour hole develops, the horseshoe vortex sinks into the scour hole and its mean size increases linearly with the depth of scour. The variation of vortex

velocity and strength with scour hole development shows increasing trends in the initial stages of scour whereas it indicates the decreasing trend in the later scouring stages.

Dey and Raikar (2007) conducted the experimental study on the turbulent horseshoe vortex in an equilibrium scour hole and intermediate stage of scour hole around a circular uniform pier of diameter 0.12 m under clear-water scour condition. The experiments were carried out in a 15 m long, 0.9 m wide and 0.7 m deep rectangular channel having uniform sediment bed of mean diameter d_{50} = 0.81 mm. The measurement of flow field and turbulence intensities were taken by an Acoustic Doppler Velocimeter (*ADV*) within the intermediate (having depth of 0.25, 0.5 and 0.75 times of the equilibrium scour depth) and equilibrium scour depth at the upstream of pier. The flow measurements were also taken in an equilibrium scour hole around the square pier with side facing the approach flow for the purpose of comparison with the uniform circular pier. They presented the contours of time averaged velocities, turbulence intensities and Reynolds' stresses at different vertical planes for developing and established equilibrium scour hole. On the basis of study they concluded that,

(a) There exist a core of higher magnitude of turbulence intensities and Reynolds stresses that increases with the development of the scour hole.

(b) The magnitude of bed shear stress at the upstream of the pier are generally greater and lower (almost equal) than the critical bed shear stress in the intermediate and equilibrium scour holes.

(c) For square pier the flow, turbulence and stress parameters are greater than those for a circular pier in an equilibrium scour hole.

2.3 CONCLUDING REMARKS

The following conclusions are drawn on the basis of the review of literature made above.

a) The flow field around a pier presents the picture of a complex phenomenon. A detailed description of the flow modified by the presence of pier in the flow is essential to control and make realistic estimation of the scour depth around the piers. Several empirical and semi-empirical relations are available for computation of scour depth around the uniform and the non-uniform piers. But many times predictions by these are not realistic. A lack of understanding of the flow pattern around the bridge piers is the main reason of this problem. Correct understanding of the flow pattern around the bridge piers therefore, is essential. A vast amount of literature is available on the topic of scour around circular uniform piers, where as less number of studies were conducted to investigate the flow pattern around such piers. The flow pattern around the circular compound piers is not yet investigated. Such geometries of bridge foundations are however, mostly used in bridge structures in the Indian-subcontinent.

b) Only a few investigators have studied the process of scour involving circular compound piers. No effort has been made as yet for investigating the temporal evolution of scour around circular compound piers; a geometry frequently adopted by the practitioners for bridge designs in India.

Thus there is an urgent need for carrying out new investigations regarding the flow pattern around the circular uniform piers.

Chapter 3

EXPERIMENTAL SET-UP AND PROCEDURE

3.1 GENERAL

Extensive data are available in literature on depth of scour around circular uniform piers. A little information however, is available on flow structure around circular uniform piers with or without scour hole. Sufficient data are also not available on temporal variation of scour depth and maximum scour depth around circular compound piers. Therefore, it is intended to study the flow pattern and temporal variation of scour depth around circular uniform pier and circular compound piers during the present investigation. Keeping this in view experiments were planned and conducted in the fluvial Hydraulics Laboratory of the Department of Civil Engineering, Jay Pee University of Information and Technology, wakhnaghat. The present chapter contains the description of the material, equipment used and the experimental procedure adopted for the investigation.

3.2 DETAILS OF EXPERIMENTAL SET-UP

3.2.1 Flume

The experiments will be conducted in a 10.0 m long, 0.75 m wide, and 0.60 m deep flume under carefully controlled conditions in the Hydraulics Laboratory of Civil Engineering, Department of Jaypee University of Information Technology Waknaghat. It will be attempted to collect data through experimentation over a wide range of pertinent variables. A working section in the flume is 3.0 m long, 0.75 m wide and 0.3 m deep, which is located 4.0 m downstream of the flume entrance. The working section will be filled with the desired sediment to the level of the flume bed. The general view of the channel is shown in Fig. 3.1 and its principal components are presented here. The water circuit is a closed loop in which clear-water is

circulated. The water can be pumped from the sump having maximum discharge capacity equal to 0.65 m^3/s. It follows the hydraulic circuit (3), and enters to the flume by passing through the channel inlet-basin. After the inlet basin, a type of honeycomb is provided at the upstream end of the flume to minimize the disturbance in the flow entering the flume. To make the flow parallel to the flume walls, flow straightners are provided just downstream of the grid at the upstream end of the flume. Boulders are filled from flume entrance to 0.5 m length towards downstream to minimize the disturbance in the flow entering the flume.

An adjustable wooden gate is provided at the downstream end of the flume to enable adjustment of the depth of the flow in the flume. Adjustable rails and trolleys are mounted on the two walls of the flume to carry the pointer gauge and other equipment used for measurements of flow pattern, water surface and bed level.

3.2.2 Sediment

River sediment retained and passed between two successive sieves will be used in all the experiments as the sediment. Generally river bed is composed of fine sediment. Keeping in mind two such uniform size non-cohesive river bed sediment having uniform size = 0.4 mm and1.8 mm will be used in all the experiments as the sediment having relative density of 2.65.

The size distribution curves for the sediment used are shown in Fig. 3.2.

3.2.3 Piers

A model of circular uniform pier was prepared using concrete. Circular uniform pier of uniform section having diameter 115 mm was used.

3.3 MEASURING INSTRUEMENTS

3.3.1 Discharge Measurement

A sharp crested orifice was provided at the downstream of the flume. The calibration curve for this sharp crested orifice was established by Kumar, (2012). The same was verified and used for the determination of discharge during the present experiments. However, value of flow discharge (Q) = 0.049 m^3/s was used herein.

3.3.2 Acoustics Doppler Velocimeter (*ADV*)

The instantaneous three-dimensional velocity components will be measured by using an "Acoustics Doppler Velocimeter**"** **(***ADV*) developed by NORTEK/SONTEK. Acoustic Doppler Velocimeters are capable of reporting accurate instantaneous values of flow velocity in three directions (Kraus *et al*., 1994; Lohrmann *et al*., 1994; Voulgaris and Trowbridge, 1998; Lopez and Garcia, 2001).

The velocity measurements will made by using Nortek A*DV* at a frequency of 25 *Hz* in a small sampling volume (approximately 0.085 cm^3) which was 5 cm away from the sensing elements. The sample volume can be described roughly as a cylinder with diameter around 6 mm and a height of 3 mm. Measurements were taken by using the down looking probe of the *ADV*.

The instrument consists of three modules: the measuring probe, the conditioning module, and the processing module. The measuring probe consists of a sound emitter transducer and three sound receiver transducers. The sound emitter generates an acoustic signal that is reflected back by sound-scattering particles present in the water, which are assumed to move with the same velocity as of water. The scattered sound signal is detected by the receivers and the flow velocity in the three directions is calculated. The *ADV* processing module consisted of a PC card, installed in a PC, and a data acquisition program.

Comparison of data obtained using the *ADV* probe and a Laser Doppler Velocimeter shows good agreement in shape and peak of the oscillatory signals from the two instruments (Kraus *et al*., 1994).

(a) Working of Micro ADV

The instrument consists of three modules: the measuring probe, the conditioning module, and the processing module. The measuring probe consists of a sound emitter transducer and three sound receiver transducers. The sound emitter generates an acoustic signal that is reflected back by sound-scattering particles present in the water, which are assumed to move with the same velocity as of water. The scattered sound signal is detected by the receivers and the flow velocity in the three directions is calculated. The *ADV* processing module consisted of a PC card, installed in a PC, and a data acquisition program.

3.3.3 Scour Depth Measurement

The temporal variation of scour depth at the nose of the pier will be measured with the help of a pointer gauge, having a least count of 0.1mm.

3.4 EXPERIMENTAL PROCEDURE

In view of the objectives of the present study, following two series of experiments were conducted. The first series of experiment were conducted to measure the flow structure around the circular uniform bridge pier. In the second series of experiments, the

observation for the temporal variation of scour depth around uniform circular bridge pier was taken. All the experiments were run under clear-water condition.

3.4.1 Flow Field Measurement Around the Bridge Pier

(a) Experimental details

The first series of experiments were carried out to investigate the three dimensional flow field around the piers. A total of 2 experiments were performed. Two experiments (run; *UPSH* and *UPRB*) were performed with piers placed on stabilized scour hole and rigid bed. The channel bed was stabilized for this purpose by spraying cement over the sediment surface. The scour hole was allowed to develop before taking observations for the flow field. For flow field measurements the uniform circular pier used had a pier diameter of 115 mm. In the remaining experiment bed was stabilized using cement without scour hole, Such run is referred as the rigid bed run. The details of these experiments are summarized in Table 4.2.

Before start of experimentation, a preliminary run was performed without the pier in place. A discharge Q of 0.049 m^3/s and flow depth h of 130 mm was determined such that sediment particles in the test section were subjected to the condition of threshold of their motion.

Table 3.1: Specifications of pier models used for both runs

Experiment	Nature of bed	b (mm)	b_* (mm)	Y
UPRB	Rigid	115	-	-
UPSH	Mobile	115	-	-

The vertical distribution of the time-averaged velocity were measured in the test section much upstream of the pier. This yielded the average approach velocity U_∞ of flow equal to 0.28 m/s. The shear velocity u_* of the approach flow was obtained through the law of the wall. The critical shear velocity u_{*c} for the corresponding grain size was determined by Shields' diagram. The clear-water condition prevailed during the experiment as u_*/u_{*c} value was ≤ 1 ($u_*/u_{*c} = 0.97$). The hydraulic parameters used for the experiment are summarized in Table 4.3.

For each of the experimental runs for measurement of flow pattern the working section was filled with uniform cohesion less material (sand) having size $d_{50} = 0.55$ mm. The pier model as specified in Table 4.2 was installed vertically in the middle of the test section and the flow condition described in Table 4.3 was established.

Table 3.2: Hydraulic parameters for the experiments

B (m)	S	h (m)	Q (m^3/s)	B/h	U_∞ (m/s)	F_r	d_{50} (mm)
1.0	0.000139	0.13	0.049	6.25	0.28	0.22	0.55

(b) Measurement strategy

The flow along the channel is considered to be symmetrical about the line passing through the center of the pier. The measurements were performed at the one-half area around the pier. Vertical distributions of the instantaneous velocities were obtained at the

measuring stations located at *P(r, a, z)*. Figure 4.4 shows the positions of measurement stations around the circular pier.

As already mentioned the vertical distributions of the time-averaged velocity were measured in the test section much upstream of the pier which yielded the average approach velocity U_∞ of flow equal to 0.28 m/s. On the rigid channel bed and also after stabilizing the geometry of scour hole for each run, the measurement for the flow velocity components were made in a vertical plane of symmetry at radial planes α = 0°, 45°, 90°, 135° and 180°. Here α = 0° corresponding to upstream central line of the flow. Velocity distributions at five vertical profiles at different radial distances (r) from the centre of pier *i.e.* r = 85, 115, 145, 175, 205, 255, 305 and 355 mm, were observed at each plane. The measurement of velocity distributions were taken at a vertical distance interval of 10 mm. Plate 4.5 shows the photographic view of flow measurement being taken by the *ADV*.

The *ADV* measures the velocity in a small sampling volume (approximately 0.09 cm^3) which is 5 cm away from the sensing elements. The measurements were taken at any particular point for long durations in order to ensure that observations become stationary. The measurements were made at a frequency of 10 *MHz* over duration of 4 minutes at each location. Each time series on velocity components was edited for a minimum signal to noise ratio of 17 and minimum correlation coefficient of 70%. The measurements of velocity component over the entire depth of flow were made by using one probe of the *ADV i.e.* downward looking probe.

The CD placed within the pocket inside of the back cover page of the thesis contains the data on the flow pattern procured through the use of *ADV*.

Chapter 5

ANALYSIS OF DATA AND DISCUSSION OF RESULTS

4.1 GENERAL

Detailed analysis of the data collected on flow structure around the circular uniform pier is presented in this chapter. The experiments were conducted in two series. In the first series the scour hole was allowed to develop and flow structure was measured around the pier using ADV. In the second series bed was made rigid as discussed in previous chapter, thus scour hole was not allowed to develop and flow structure was measured A detailed discussion on how flow structure alters due to the variation of bed is presented here.

4.2 Scour around circular pier

The significance of temporal variation for the determination of design scour depth is described in Chapter 2. The laboratory experiments on circular uniform piers were conducted as per details given in Chapter 3.

Temporal variation for uniform isolated pier is shown in fig 4.8 and countor for the same pier is shown in fig 4.9

4.3 Flow field around circular pier

One of the main objectives of the present investigation was to study the flow structure around the circular uniform pier for the clear-water condition with and without the

presence of scour hole around them. For this purpose an Acoustic Doppler Velocimeter (*ADV*) was used to measure instantaneously the three components of the velocity.

Measurement for the flow structure at different measuring stations around the circular uniform pier model was made as per experimental details given in Chapter 3. The flow structure comprises vertical distribution of velocity components, turbulence intensities, Reynolds' stresses and turbulent kinetic energy.

Firstly, the detailed discussions on the flow pattern around the circular uniform pier model (*UPSH*) while scour hole is allowed to develop are made. Next the comparison is presented between the flow structures observed with or without scour hole around the circular uniform pier on two vertical planes i.e $\alpha = 0^o$ and 180^o

4.3.1 Flow Field Around Circular Uniform Pier Model (*UPSH*)

In Chapter 3, the methodology for the velocity field measurement around the uniform circular pier model (*UPSH*) was explained. The measurements were made at five different vertical planes in radial directions at $\alpha = 0^o$, 45^o, 90^o, 135^o and 180^o from the flow. However detailed discussions on variation of time average velocities, turbulence intensities and Reynolds' stresses are presented only for vertical planes at $\alpha = 0^o$, 90^o and 180^o due to space limitations. A comparison with the literature data on these aspects is also made.

(a) Vertical distribution of the velocity

The variation of time averaged components of velocities (longitudinal *u*; transverse *v* and vertical *w*) in the planes at $\alpha = 0°$, 90^o and 180^o is shown in Figs. 5.1 (a - c) respectively.

The velocity components were normalized using upstream flow velocity U_∞ while the vertical distance z is normalized using depth of flow h.

In the plane at $\alpha = 0°$, *a*pproaching to the pier *i.e.* while r is small and below the level of initial bed in the scoured region the u component shows negative values, which indicates reversal of the flow near the pier. The maximum negative value of u is about 0.33 times U_∞. The v component of the velocity is negligibly small in this plane, which indicates that flow is symmetrical. Approaching to the pier, the w component of velocity has larger values in downward direction which is being considered as negative. This means there is dominancy of strong down flow in this region with maximum value of downward velocity being equal to about 0.35 times U_∞ . At the bottom of the scour hole and close to pier, w component show positive value, which indicate that there is upward motion near the bed of the scoured region. Similar results were however also obtained by Melville, (1975); Graf and Istiarto, (2002) and Dey and Raikar, (2007), Kumar and Kothyari (2012).

In the plane at $\alpha = 90°$, approaching to the pier and below the general bed level the value of u component show decreasing positive value towards the scour bed. The v component is small while $r > 165$ mm. Close to the pier and over the entire depth of flow the flow patterns of v component was similar to that in case of plane at $\alpha = 45°$. Similar flow pattern was observed by Istiarto, (2001). The w component is showing always downward flow movement in this plane as well as in the planes at $\alpha = 0°$ and 45°, but with lower intensity. This intensity of downward movement of the flow decreases as the flow moves towards the downstream side of the pier. Just below the initial bed level and close to the pier the maximum downward velocity was obtained nearly 0.35 U_∞. A similar

magnitude of downward velocity was observed by Istiarto, (2001) and Kumar and Kothyari (2012).

In the plane at α = 180°, close to the pier *i.e.* while *r* is small, the *u* component shows a reversal of flow near the water surface also far away from the pier *i.e.* while *r* is larger, the *u* component albeit is larger as compared to its value near the pier but it still has a decreasing tendency near the surface of the flow. In this wake region *i.e.* when α = 180°, the *v* component is seen to fluctuate about its mean value. The normalized value of *v* component is seen to vary between 0 and 0.55 over this plane. On the contrary to the observations at α = 0° the value of *w* component is always positive at α = 180° revealing that upward flow in the wake region. Similar observation was noticed by Graf and Istiarto, (2002) at this plane. Just behind the pier *i.e.* when *r* =85 mm, the *w* component is as large as about 0.47 U_∞ and the same is positive and hence is in upward direction.

(b) Vertical distribution of turbulence characteristics

The turbulence characteristics are represented by turbulence intensities ($\sqrt{\overline{u'u'}}$, $\sqrt{\overline{v'v'}}$, $\sqrt{\overline{w'w'}}$), Reynolds' stresses ($\overline{u'w'}, \overline{v'w'}$) and the turbulent kinetic energy (*k*) of the flow. Where u' is the fluctuation of *u* component, v' is fluctuation of *v* component and w' is fluctuation of *w* component. The results obtained are presented in Figs. 5.3 (a - c) for the some selected planes *i.e.* at α = 0º, 90º and 180º due to the space limitation. The data of turbulence intensities, Reynolds' stresses and the turbulent kinetic energy are normalized using shear velocity u_* in the approach flow.

I. Vertical distribution of turbulence stresses

In the plane at α = 0° the turbulence intensities (particularly the vertical component $\sqrt{\overline{w'w'}}$ of turbulence intensity) show no significant change in the upper zone *i.e.* when $z >$ 0 and their values decrease towards the water surface. However, there is an increase with z/h in the values of turbulence intensities within the scour hole. The longitudinal component of Reynolds' stress ($-\overline{u'w'}$) has positive values within the scour hole and near the bed. Also the longitudinal component $-\overline{u'w'}$ is dominant over transverse component $-\overline{v'w'}$ of Reynolds' stress.

In the planes at α = 45° the distribution of all the three components of turbulence intensity is similar (not shown here) as it was in the plane α = 0°. The magnitude of longitudinal component $-\overline{u'w'}$ of Reynolds' stress is slightly higher than the previous plane.

In the plane at α = 90°, all the three components of turbulence intensity show higher magnitude. This is in contrast to the results of Istiarto, (2001) who indicated that only magnitude of $\sqrt{\overline{v'v'}}$ component to be significant. Within the scoured region and below the general bed level the $-\overline{u'w'}$ component has large values in comparison to $-\overline{v'w'}$. Both components of Reynolds' stress have higher magnitude than that observed in other planes.

In the plane at α = 135° approaching to the pier, within the scoured region and below the general bed level (z < 0), the magnitudes of all the components of turbulence intensity are higher than those in the planes upstream to this. However trend of the variation is similar. Above the general bed level and far away from the scoured region, the

profile of turbulence intensity and Reynolds' stress components exhibit similar magnitudes.

In the downstream plane when α = 180°, the turbulence is seen to be more strong as compared to that in the plane upstream of the pier. Close to the pier, the magnitudes of the three components of turbulence intensity are almost two times of the corresponding values in the plane at α = 0°. As the flow moves away from the pier, the turbulence intensities are seen to decrease. The stress components $\overline{u'w'}$ and $\overline{v'w'}$ however show no conclusive trend, still their magnitudes are much higher than those in the plane at α = 0°. The direction of stress components is opposite to that in the plane at α = 0° and these are more staggered here indicating the presence of larger turbulence in the wake region.

II. Turbulent kinetic energy

The combined effect of the all the three component of the turbulence intensity can be better defined by turbulent kinetic energy of the flow defined as:

$$k = \frac{1}{2}\left(\overline{u'u'} + \overline{v'v'} + \overline{w'w'}\right) \tag{4.1}$$

The data of turbulent kinetic energy is normalized by using the shear velocity of approach flow. Figure 4.3 shows the vertical distribution of the normalized turbulent kinetic energy. The profiles of turbulent kinetic energy observed are the same as it is for the turbulence intensities. In the planes at α = 45º and 90º , above the general bed level the profiles of normalized turbulent kinetic energy show similar trend and their magnitude is almost equal. One more interesting feature is that, core of high magnitude of turbulent kinetic energy were observed almost in the middle of scour hole in these planes.

In the planes at α = 135º and 180º, a sharp increase in the magnitude of kinetic energy is observed over the entire depth of flow. Just behind the pier the intensity of magnitude being highest and then reduces as the flow moves away from the pier. The flow is highly turbulent in these planes. The magnitude of turbulent kinetic energy increases as the flow moves from the upstream plane *i.e.* at α = 0º to the downstream plane (α = 180º).

4.3.2 Comparison of the Flow Field Around Circular Uniform Pier (Run *UPRB*) with that Around the Circular uniform Pier (Run *UPSH*) Placed in Rigid Bed

The measurements of velocity, turbulence intensities and Reynolds' stresses were also made around the circular uniform pier (*UPRB*) and circular compound pier (*UPSH*) while they were placed on the rigid bed. The measurement were made around these piers at different vertical planes at radial direction at α = 0°, 45°, 90°, 135° and 180° . However discussions on time average velocities, turbulence intensities and Reynolds' stresses are made here only for data of planes α = 0º and 180º due to the space limitation.

(a) Measurement in the plane at α = 0°

Figures 4.4 (a - c) depict the vertical distribution of time averaged velocity components (*u*, *v*, *w*) of the experimental runs *UPRB* and *UPSH*. The longitudinal velocities are normalized by approach flow velocity while vertical spacing is normalized by flow depth. From the data comparison it becomes clear that no significant change occurred in the value of *u, v* and *w* components of the velocity between these two experimental runs over the entire depth of flow and over the entire region of measurement. The distribution of *u* component is uniform for entire depth of flow. The magnitude of *v* component is negligible over the entire depth of flow for both the experimental runs. The maximum

down flow is observed at r/r_p = 0.91 and it is about 0.04 U_∞ for the experimental run *UPRB*. Here r_p is the radius of the pier. However this value is smaller than that observed by Graf and Yulistiyanto, (1998) and Ettema, (1980). Graf and Yulistiyanto measured the *w* component having magnitude about 0.3 U_∞ at r/r_p = 1.1.

Figures 4.5 (a - d) show the comparison of vertical distribution of normalized turbulence intensities ($\sqrt{\overline{u'u'}}$, $\sqrt{\overline{v'v'}}$, $\sqrt{\overline{w'w'}}$) and normalized Reynolds' stresses ($\overline{u'w'}$, $\overline{v'w'}$) for the plane at α = 0º. No significant change is observed in the profiles of $\sqrt{\overline{u'u'}}$ and $\sqrt{\overline{w'w'}}$ over entire region of measurement. However close to the pier while *r* < 175 mm, the component $\sqrt{\overline{v'v'}}$ is noticed to be higher in magnitude for the experimental run *UPRB*. The Reynolds' stress components ($\overline{u'w'}$, $\overline{v'w'}$) show no appreciable change in their values due to the presence of top of the foundation. Results similar to these were also noticed at the other planes of observations in the upstream half of the piers.

(b) Measurement in the plane at $\alpha = 180°$

The comparison of vertical distribution of time averaged velocity components (*u*, *v*, *w*) for the plane at α = 180º are given in Figs. 4.6 (a - c). With regard to the *u* component of velocity; approaching to the pier when *r* < 255 mm, flow reversal towards the water surface was observed for both the experimental runs. This tendency of flow reversal increases close to the pier. However, magnitude of *u* component of velocity was noticed to be smaller for the experimental run *UPSH*. Far away from the pier while *r* > 305 mm; *u* component has positive value over the entire depth of flow. The *v* component exhibits the

transverse movement along the depth of flow. This tendency of transverse movement is noticed to be higher for the experimental run *UPRB*. The *w* component is observed to be positive for the experimental run *UPSH i.e*. flow direction is towards the water surface. For the experimental run *UPRB*, just behind the pier, *w* component show downward (negative) component while this downward component is not noticeable in the case of *UPSH* run.

Figures 4.7 (a - d) give the comparison of vertical distribution of normalized turbulence intensities ($\sqrt{\overline{u'u'}}$, $\sqrt{\overline{v'v'}}$, $\sqrt{\overline{w'w'}}$) and normalized Reynolds' stresses ($\overline{u'w'}$, $\overline{v'w'}$) for the plane at α = 180º. The data of both the experimental runs present the highly scattered profiles of the turbulence intensity components and Reynolds' stress components over the entire region of measurement. The data is less organized in this wake region due to the highly turbulent zone. The non-uniform distributions of the data in this region indicate that larger time duration is needed for measuring the velocity fluctuations in the wake region of flow.

Chapter 5
CONCLUSIONS

5.1 GENERAL

Broad objectives of the present investigation were: (i) to study the flow structure around the circular uniform pier for the clear-water scour condition placed in rigid bed as well as in the scour hole, (ii) to study the comparison of flow structure of uniform pier in rigid bed run and with scour hole run in the context of engineering practice in the Indian sub-continent was discussed initially.

Keeping in mind the broad objectives, two series of experiments were conducted in the laboratory for collecting the relevant data. In the first series experiments were conducted for a better understanding of the flow and the turbulence characteristics around the circular uniform pier placed on the rigid bed and in the scour hole. The second series of experiments was conducted to compare the data of flow structure around uniform pier in scour hoe condition and as well as uniform pier without scour hole, both the runs were carried out in rigid bed condition for clear-water condition. Laboratory data already collected by other investigators on this topic were also used for the purpose of analysis.

The following general conclusions can be drawn based on this study:

(a) The horseshoe vortex can be considered as the basic mechanism causing scour around the bridge piers.

(b) The flow characteristics around the circular uniform pier in scour hole are moreover same as compared to the flow characteristics around the circular uniform pier without scour hole.

(c) The specific conclusions arrived at are summarized below.

5.2 FLOW FIELD AROUND CIRCULAR PIER

Well controlled measurements were taken with the help of Acoustic Doppler Velocimeter (*ADV*) on the flow characteristics around circular uniform pier placed on the rigid bed and in the scour hole. Detailed measurements regarding the time averaged velocity components (u, v and w), turbulence intensity components and Reynolds' stress components were made around the pier at vertical planes in different radial directions with α = 0º, 45º, 90º, 135º and 180º. The flow structure around the circular uniform pier placed in rigid bed and in the scour hole were compared for two vertical planes α = 0º and 180 º

5.2.1 Flow Field Around Circular Uniform Pier (*UPSH*)

The followings features related to the flow field around uniform pier were noticed from the experiments.

(a) On upstream plane of the pier at α = 0º, a maximum downward velocity about $0.35U_\infty$ occurs close to the pier.

(b) On upstream of the pier at α = 0º, a circular rotating vortex close to the pier was noticed which is commonly known as the principal vortex of the horseshoe vortex system. Such vortex system was also noticed to occur at plane α = 45º. However the size of the vortex was significantly smaller in the plane at α = 90º.

(c) On the downstream plane *i.e.* at α = 180º, flow reversal towards the water surface was noticed. The less organized data on turbulence in the downstream plane (α = 135º) indicated the flow to be highly turbulent in the wake region. As the flow

moves from the upstream towards the downstream planes the turbulence in the flow increases.

5.2.2 Comparison of the Flow Field Around Circular Uniform Pier Placed in Rigid Bed (Run *UPRB*) with that Around Circular uniform Pier Placed in scour hole Bed (Run *UPSH*)

(a) In the plane at $\alpha = 0^{o}$ no significant change was noticed in the values of *u, v* and *w* components of the velocity between these two experimental runs over the entire depth of flow and over the entire region of measurement. Similarly no significant change is observed in the profiles of $\sqrt{\overline{u'u'}}$ and $\sqrt{\overline{w'w'}}$ over entire region of measurement. However close to the pier while $r < 125$ mm, the component $\sqrt{\overline{v'v'}}$ is noticed to be higher in magnitude for the experimental run *UPRB*. The Reynolds' stress components show no appreciable change in their values due to the presence of top of the foundation. Results similar to these were also noticed at the other planes of observations in the upstream half of the piers.

(b) At the plane at $\alpha = 180^{o}$, for *u* component of velocity; flow reversal towards the water surface was noticed for both the experimental runs. However, magnitude of *u* component of velocity was noticed to be smaller for the experimental run *UPSH*. The *v* component exhibits the transverse movement along the depth of flow. This tendency of transverse movement is noticed to be higher for the experimental run *UPRB*. The *w* component is observed to be positive for the experimental run *UPRB i.e.* flow direction is towards the water surface in this case. For the experimental run *UPSH*, just behind the pier, *w* component show downward (negative) component while this downward component is not noticeable in the case of *UPSH* run. The

data of both the experimental runs present the highly scattered profiles of the turbulence intensity components and Reynolds' stress components over the entire region of measurement in the wake region. The data is less organized in this wake region due to the highly turbulent wake zone.

REFERENCES

Ahmed, F., and Rajaratnam, N. (1998). "Flow around bridge piers." J. of Hydr. Engg., ASCE, Vol. 124, No. 3, pp 288-300.

Ahmed, F., and Rajaratnam, N. (2000). "Observations on flow around bridge abutments." J. of Engg. Mech., Vol. 126, No.1, pp 51-59.

Ali, K. H. M., Karim, O. A., and O'Connor, B. A. (1997). "Flow patterns around bridge piers and offshore structures." Proc., 27th IAHR Congress, San Francisco, California, Theme A, pp 208–213.

Breusers, H. N. C., Nicollet, G., and Shen, H. W. (1977). "Local scour around cylindrical piers." J. of Hydr. Res., IAHR, Vol. 15, No. 3, pp 211-252.

Breusers, H. N. C., and Raudkivi, A. J. (1991). "Scouring." Hydraulic Structures Design Manual, No. 2, A. A. Balkmea, Rotterdam, The Netherlands.

Garde, R. J., and Ranga Raju, K. G. (2000). "Mechanics of sediment transportation and alluvial stream problem." New Age International, New Delhi.

Graf, W. H., and Istiarto, I. (2002). "Flow pattern in the scour hole around a cylinder." J. of Hydr. Res., IAHR, Vol. 40, No.1, pp 13-20.

Kothyari, U. C. (1989). "Scour around bridge piers." Ph.D. Thesis, Indian Institute of Tech. Roorkee (Formerly: Univ. of Roorkee, Roorkee), India.

Kraus, N. C., Lohrmann, A., and Cabrera, R. (1994). "New acoustic meter for measuring 3D laboratory flows." J. of Hydr. Engg., ASCE, Vol. 125, No. 3, pp 406-412.

Lohrmann, A., Cabrera R., and Kraus, N. (1994). "Acoustic doppler velocimeter (ADV) for laboratory use." Proc. Symp. on Fundamentals and Advancements in Hydr. Measurements and Experimentation, ASCE, New York, pp 351–365.

Lopez, F., and Garcia, M. H. (2001). "Mean flow and turbulence structure of open-channel flow through nonemergent vegetation." J. of Hydr. Engg., ASCE, Vol. 127, No. 5, pp 392-402.

Melville, B. W., and Raudkivi, A. J. (1977). "Flow characteristics in local scour at bridge sites." J. of Hydr. Res., IAHR, Vol. 15, No. 4, pp 373-380.

Olsen, N. R. B., and Kjellesvig, H. M. (1998). "Three-dimensional numerical flow modeling for estimation of maximum local scour depth." J.of Hydr. Res., IAHR, Vol.36, No.4, pp 579-590.

Richardson, J. E., and Panchang, G. P. (1998). "Three-dimensional simulation of scour-inducing flow at bridge piers." J. of Hydr. Engg., ASCE, Vol. 124, No. 5, pp 530-540.

Kumar.A[1](2012). "Comparative study of Three-dimensional flow characteristics at exposed non uniform circular pier Hydrauics and water resource (HYDRO 2012) IIT Bombay, India

Kumar, A., and Kothyari, U. C., 2012. Three-dimensional flow characteristics within the scour hole around circular uniform and compound piers, J. of Hydr. Eng., 138 (5), 420-429.

Kumar, A., and Kothyari, U. C., 2005. Flow Characteristics within Scour Hole around a Circular Bridge Pier, Proc. Conf. on Hydraulics and Water Resources-HYDRO 2005, Tumkur, India, 599-608.

Kumar, A., 2007. Scour around circular compound bridge piers, Ph.D. Thesis, Indian Institute of Tech., Roorkee, India.

Kumar, A., 2010. Experimental data of flow characteristics around the circular uniform and compound bridge piers using acoustic Doppler velocimeter,

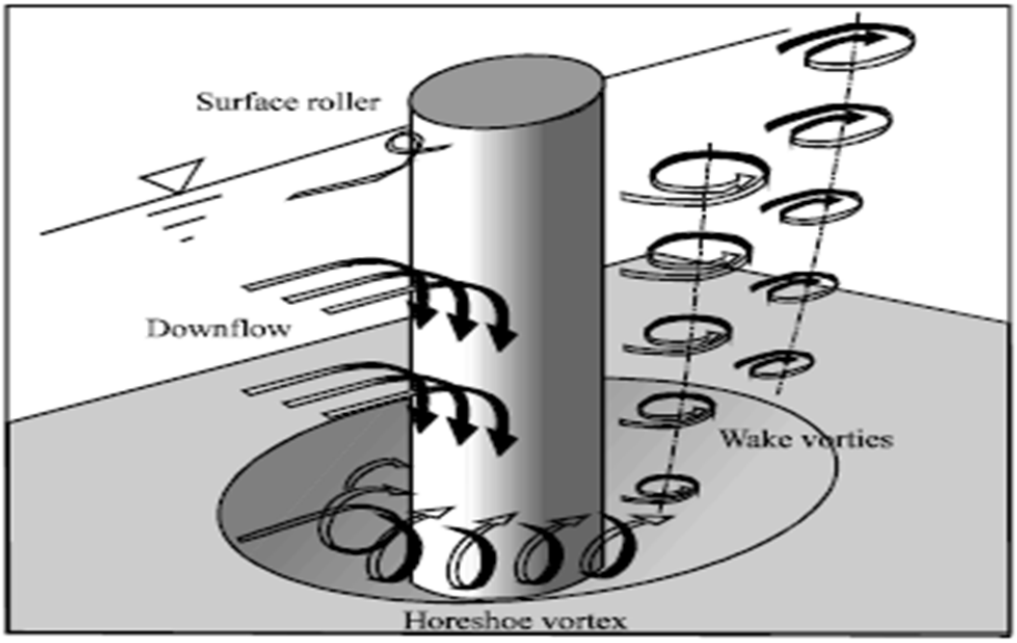

Fig 1.1: Mechanism of scour(Raudkivi,1990)

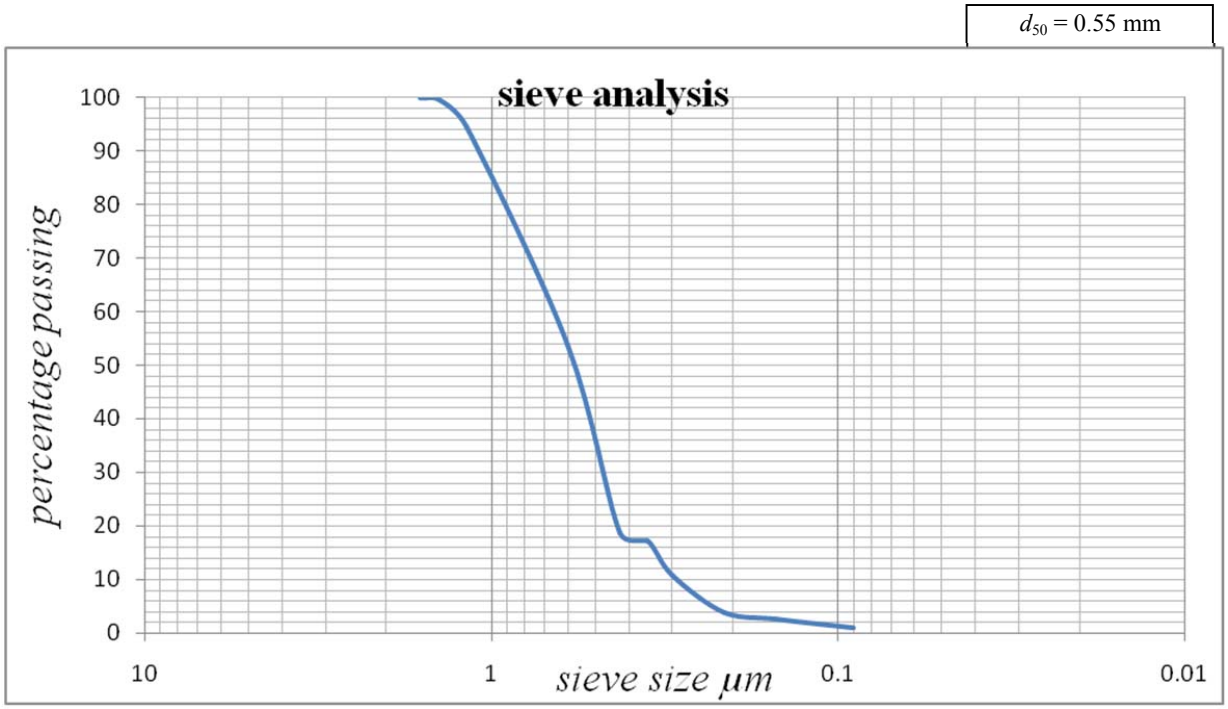

FIG. 3.2: Grain size distribution curves of sediments used

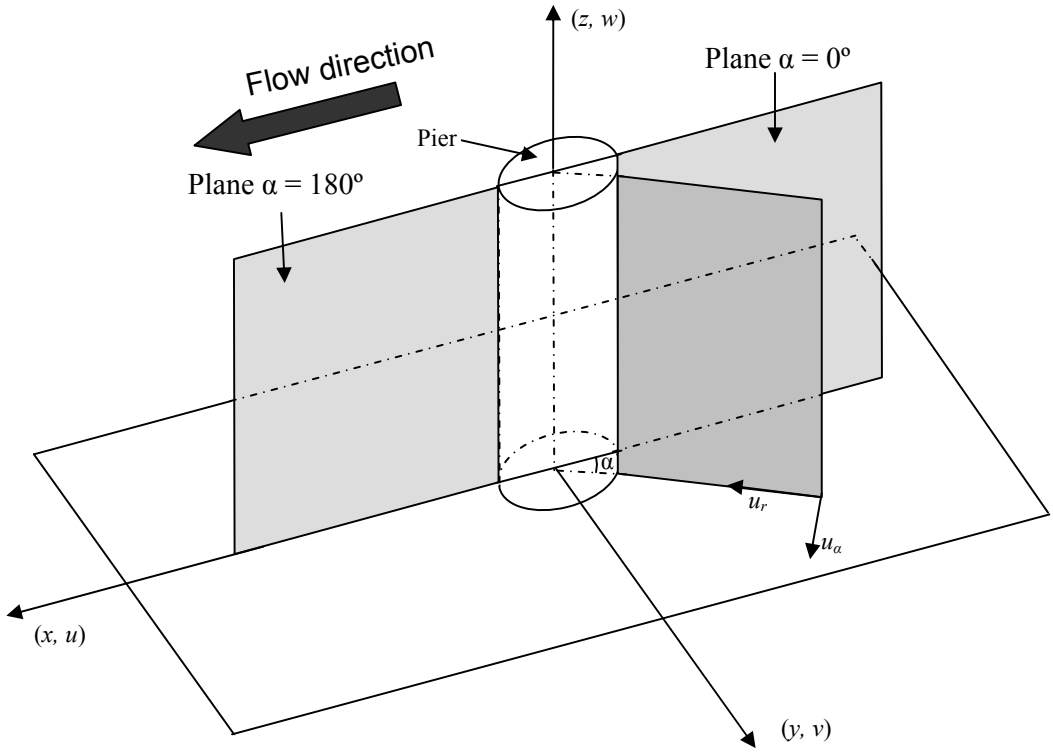

FIG. 4.3: Cartesian and cylindrical coordinate systems (Kumar, 2007)

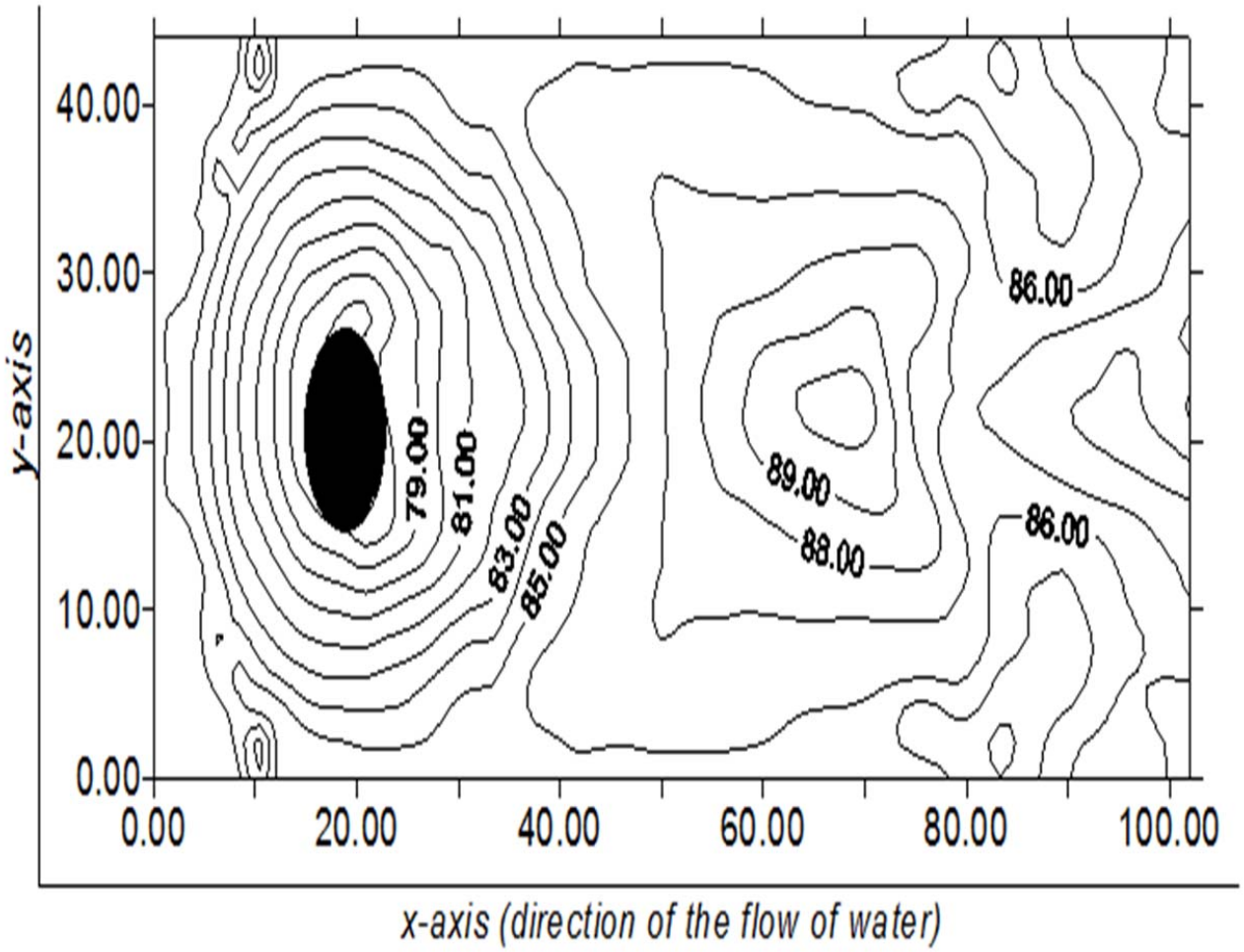

Fig no 4.9: Contouring uniform isolated circular pier

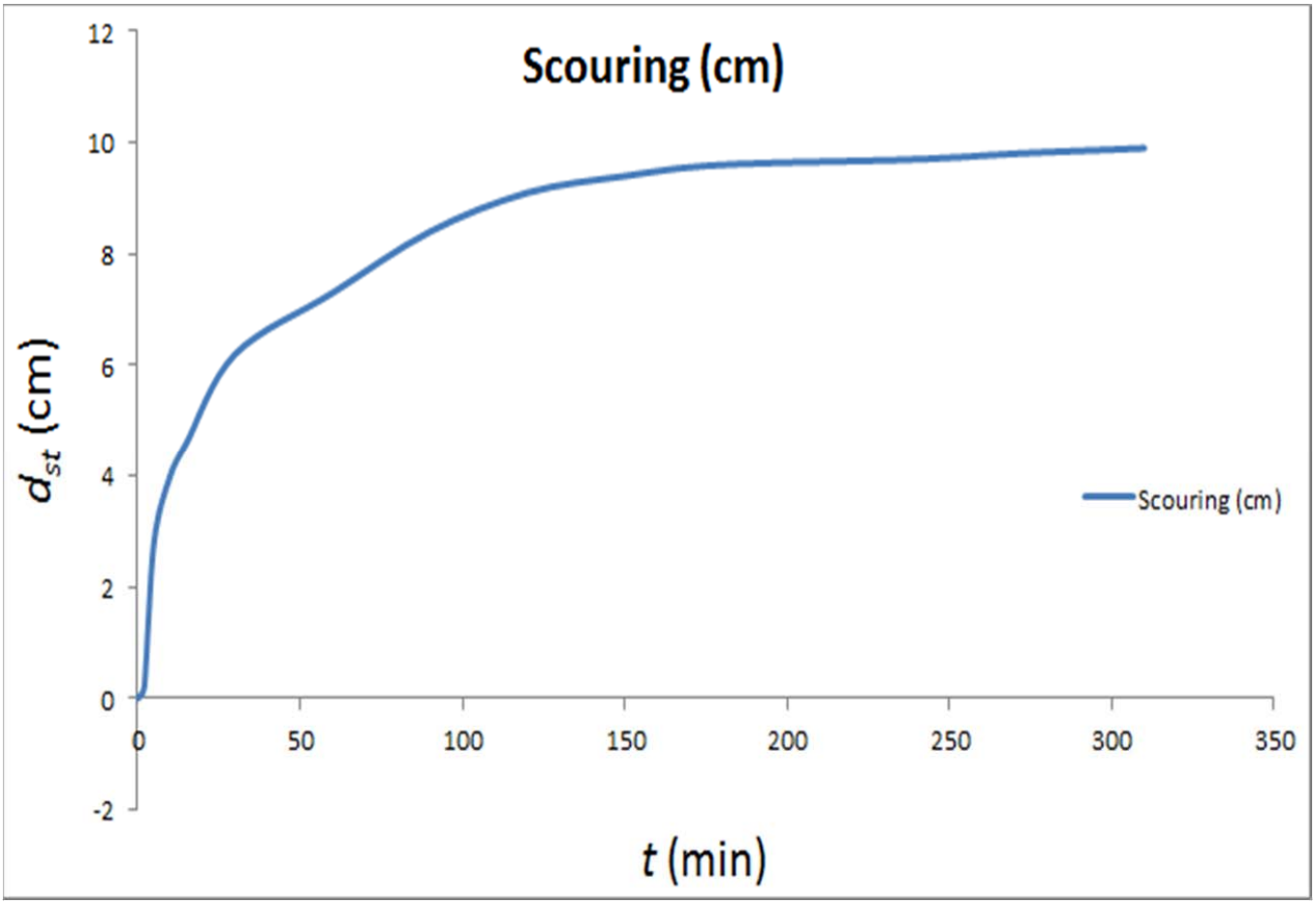

Fig no 4.8: Temporal variation for uniform circular bridge pier

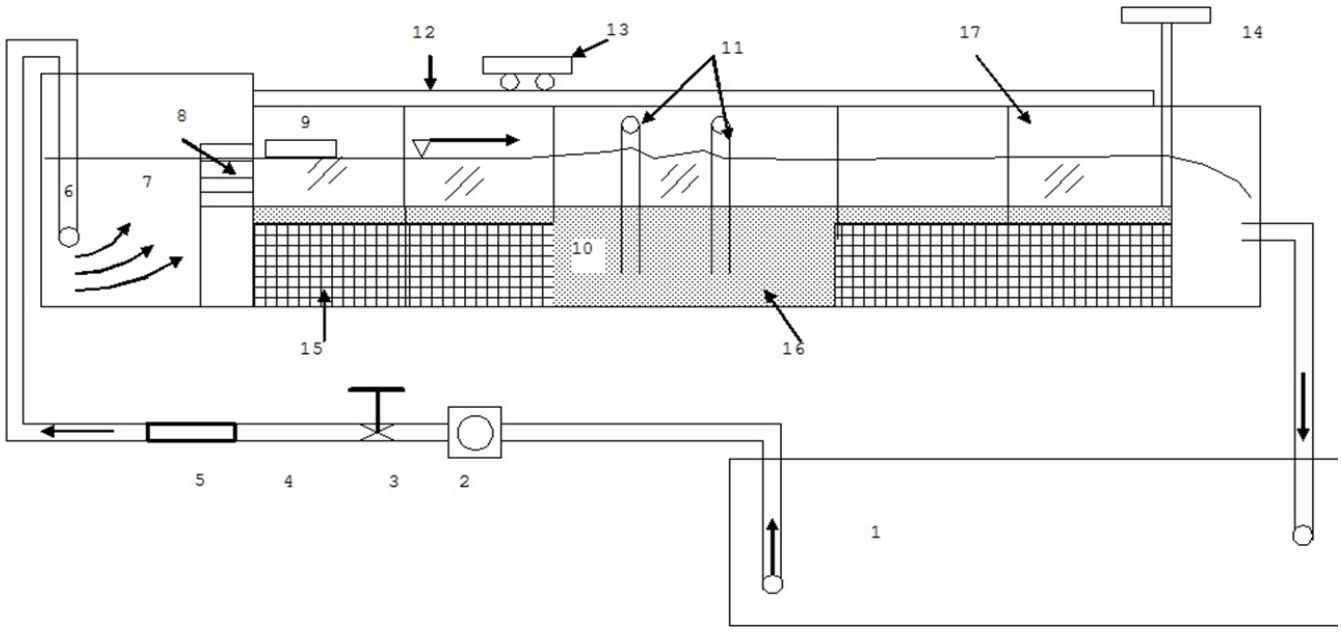

1 water sump
2 pump
3 operative valve
4 hydraulic circuit
5 orifice meter
6 inlet pipe
7 inlet basin
8 honey-comb
9 floating plate
10 Working section
11 piers
12 railing
13 trolly
14 tail-gate
15 masonary
16 sediment
17 glass side of flume

FIG 3.1: Schematic diagram of Experimental set-up (Open channel flume)

FIG. 4.1 (a): Normalized profiles of *u, v* and *w* component of velocity measured around the circular uniform pier (*UPSH*) at plane α = 0º

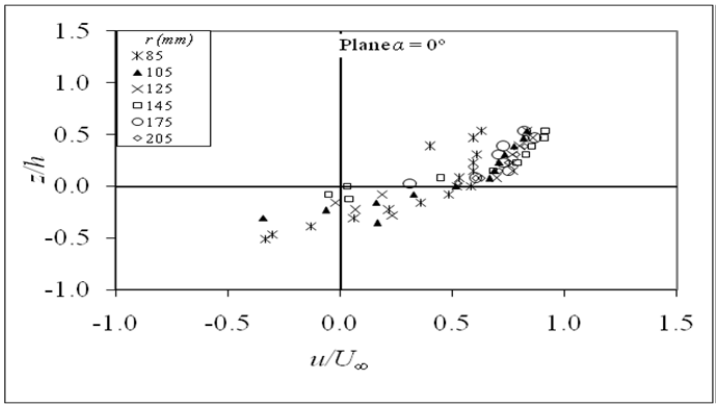

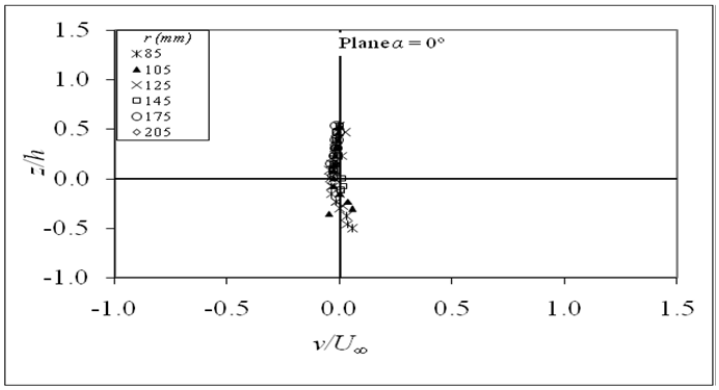

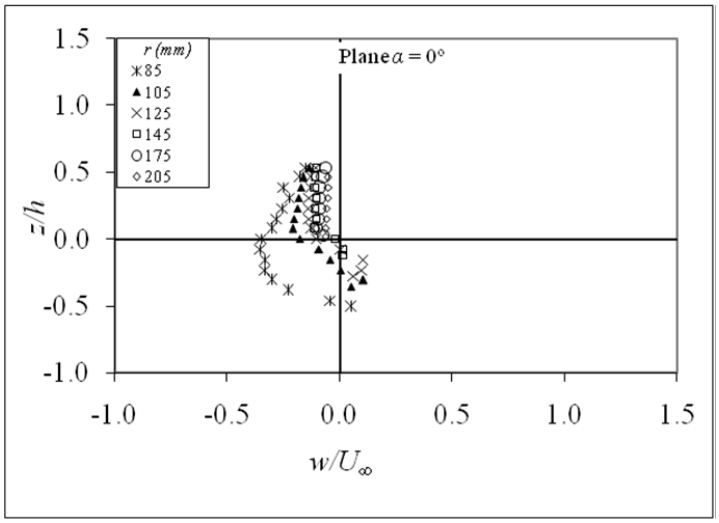

FIG. 4.1 (b): Normalized profiles of *u*, *v* and *w* component of velocity measured around the circular uniform pier (*UPSH*) at plane

$\alpha = 90^{o}$

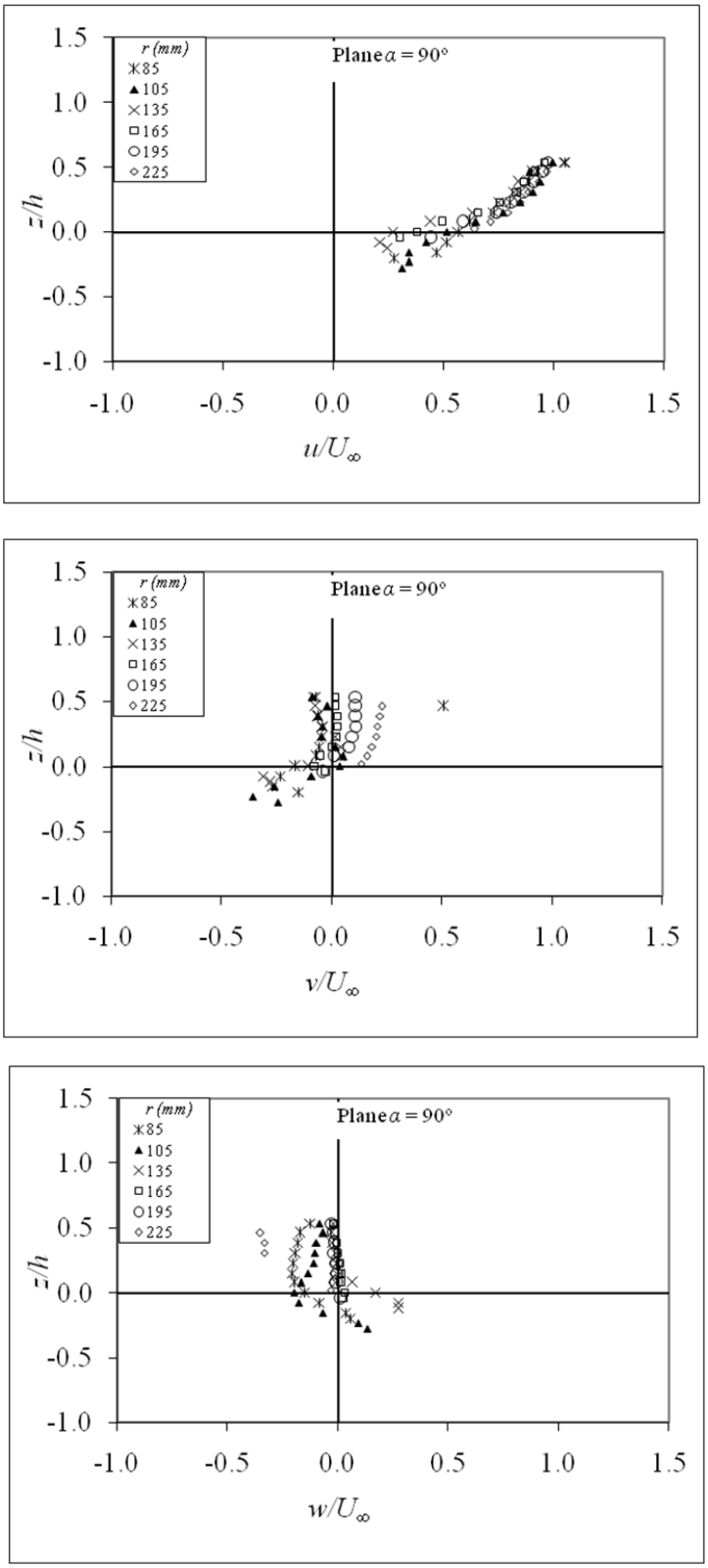

FIG. 4.1 (c): Normalized profiles of *u*, *v* and *w* component of velocity measured around the circular uniform pier (*UPSH*) at plane α = 180º

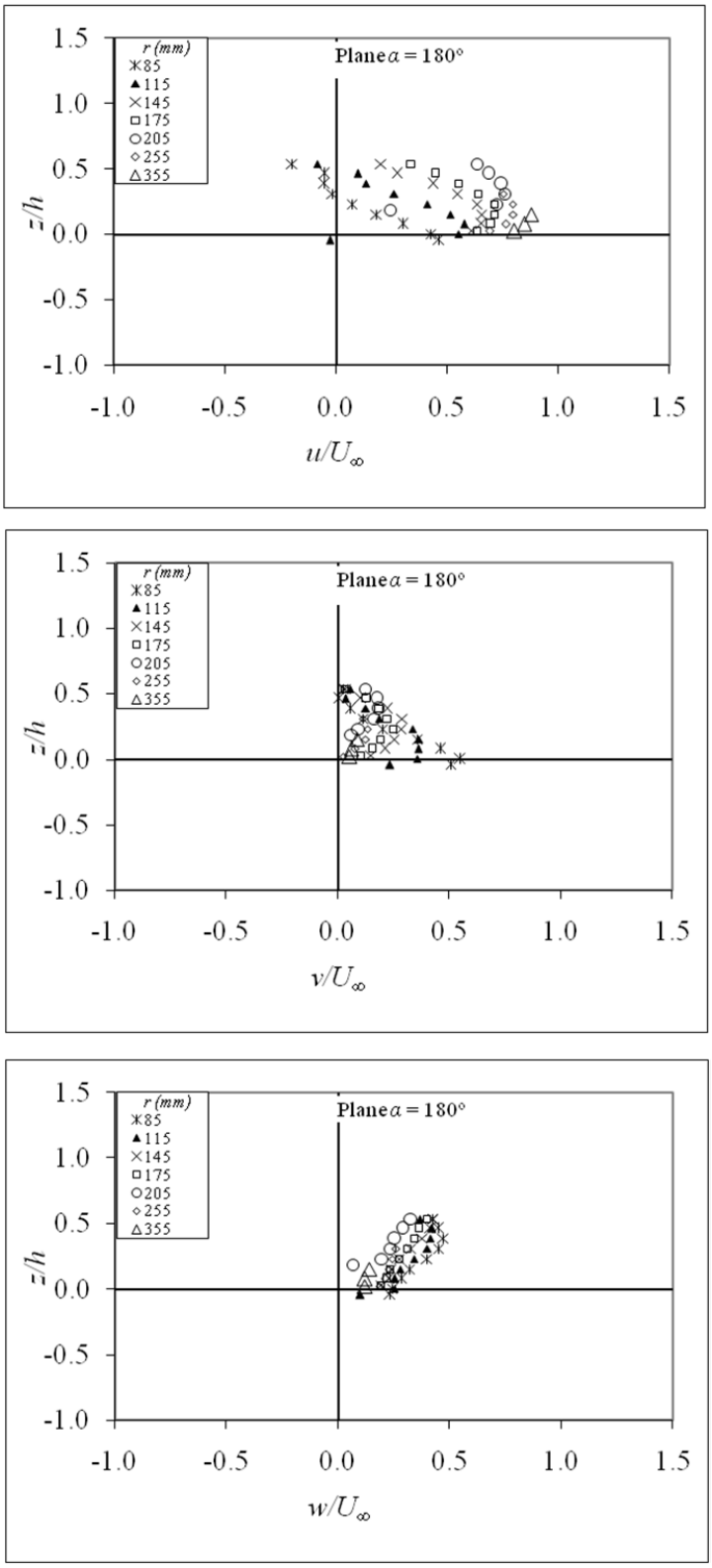

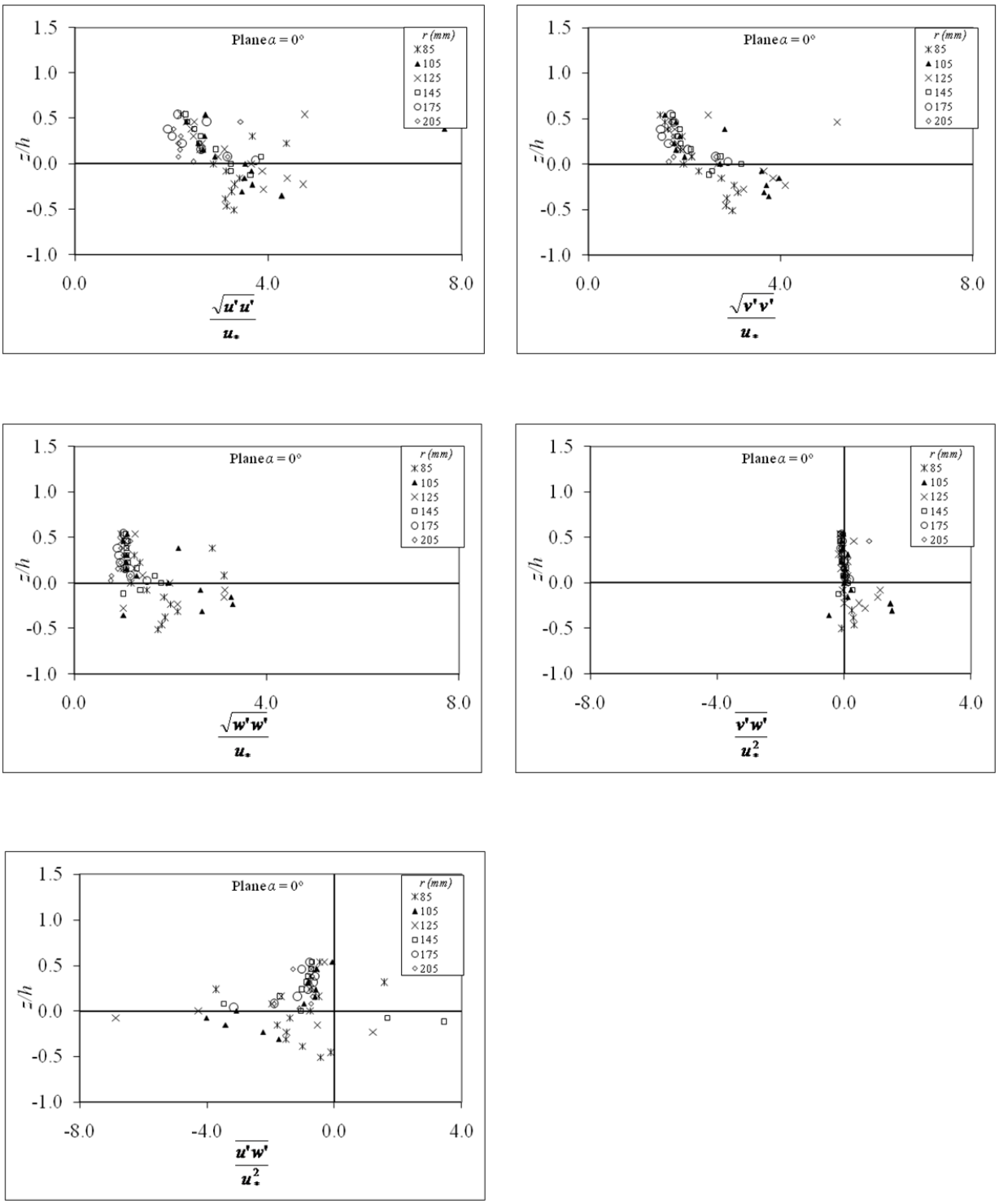

FIG. 4.2 (a): Normalized profiles of components of turbulence intensity and Reynolds' stresses measured around the circular uniform pier (*UPSH*) pier at plane α = 0º

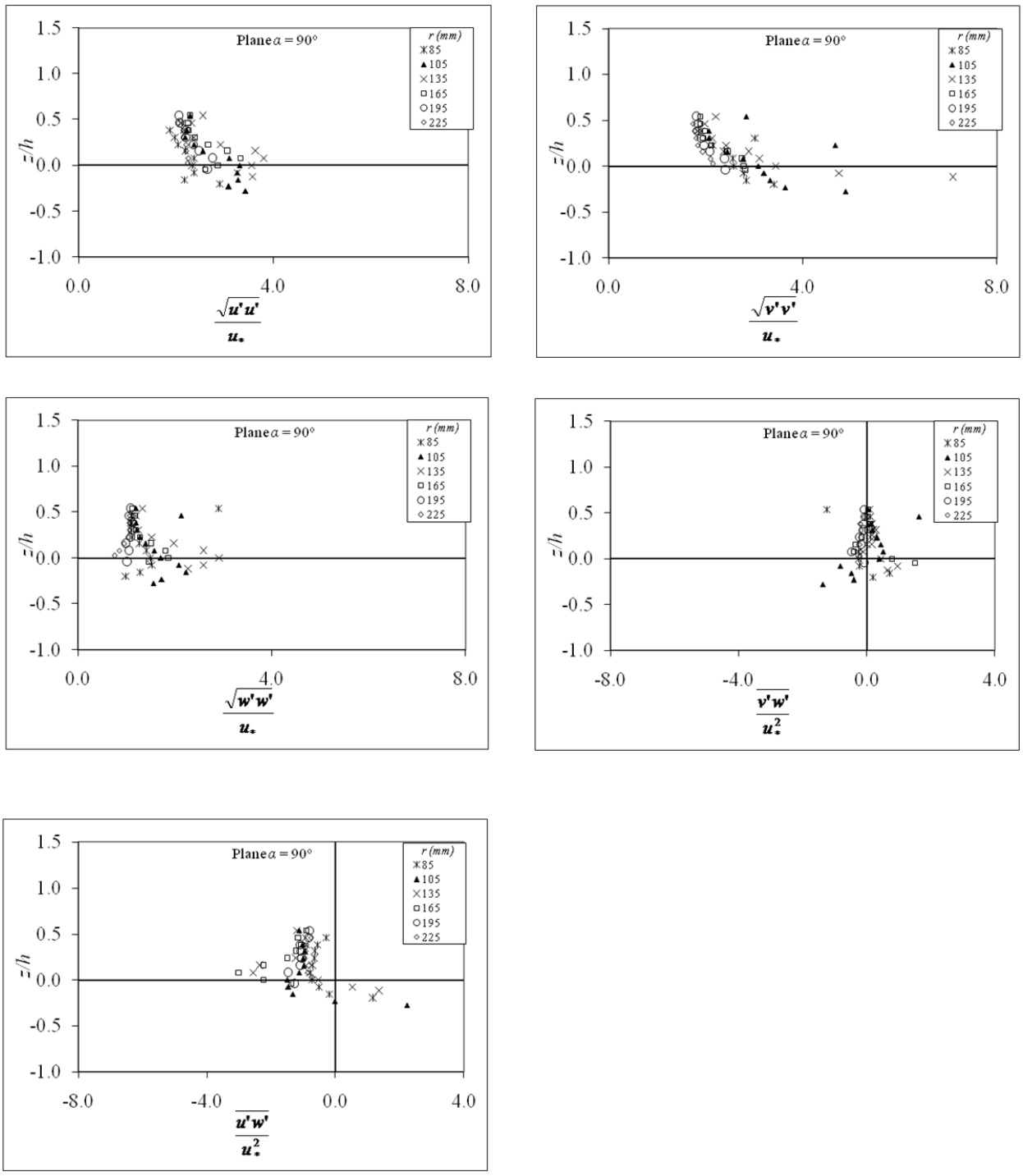

FIG. 4.2 (b): Normalized profiles of components of turbulence intensity and Reynolds' stresses measured around the circular uniform pier (*UPSH*) pier at plane α = 90º

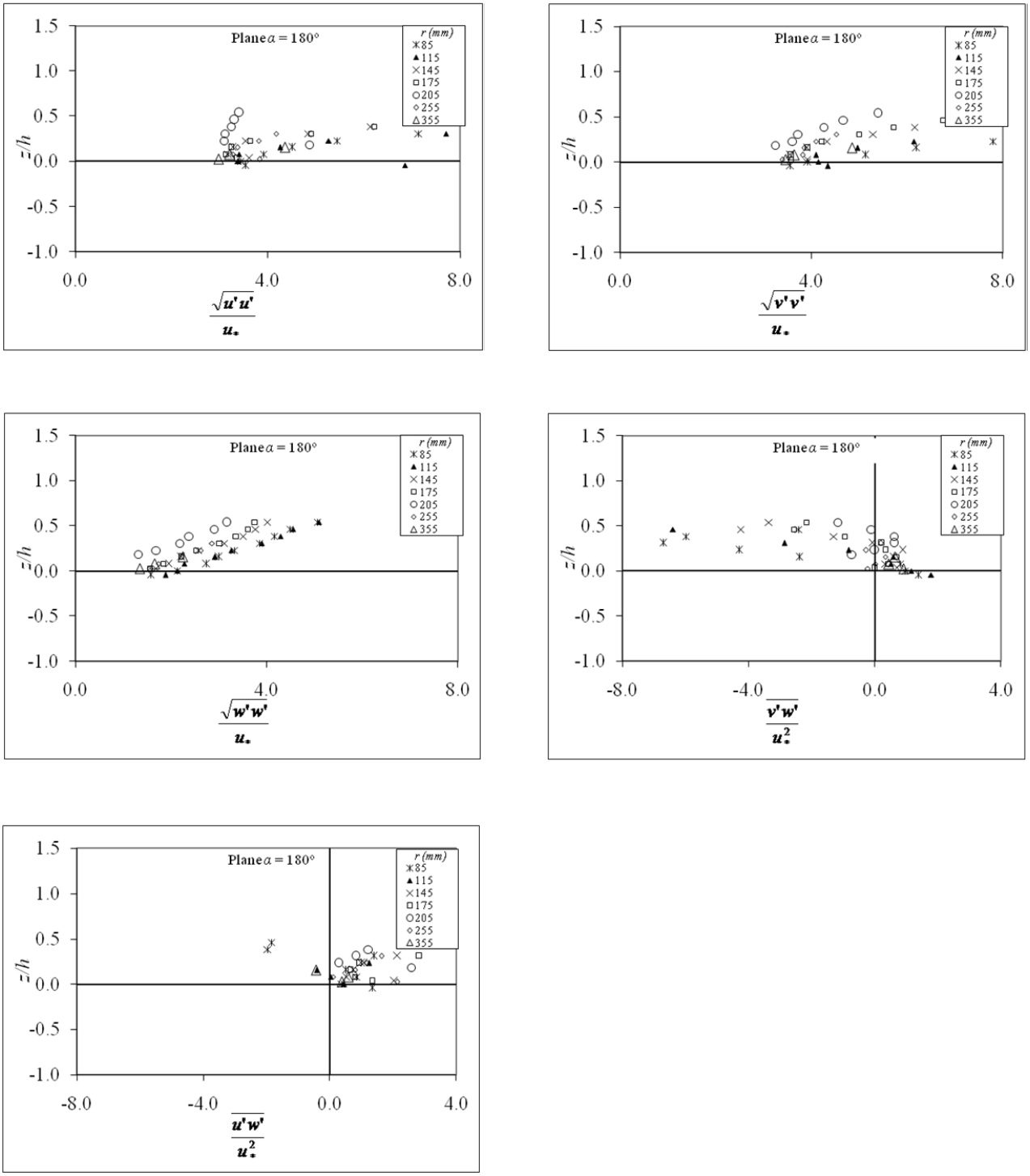

FIG. 4.2 (c): Normalized profiles of components of turbulence intensity and Reynolds' stresses measured around the circular uniform pier (*UPSH*) pier at plane α = 180º

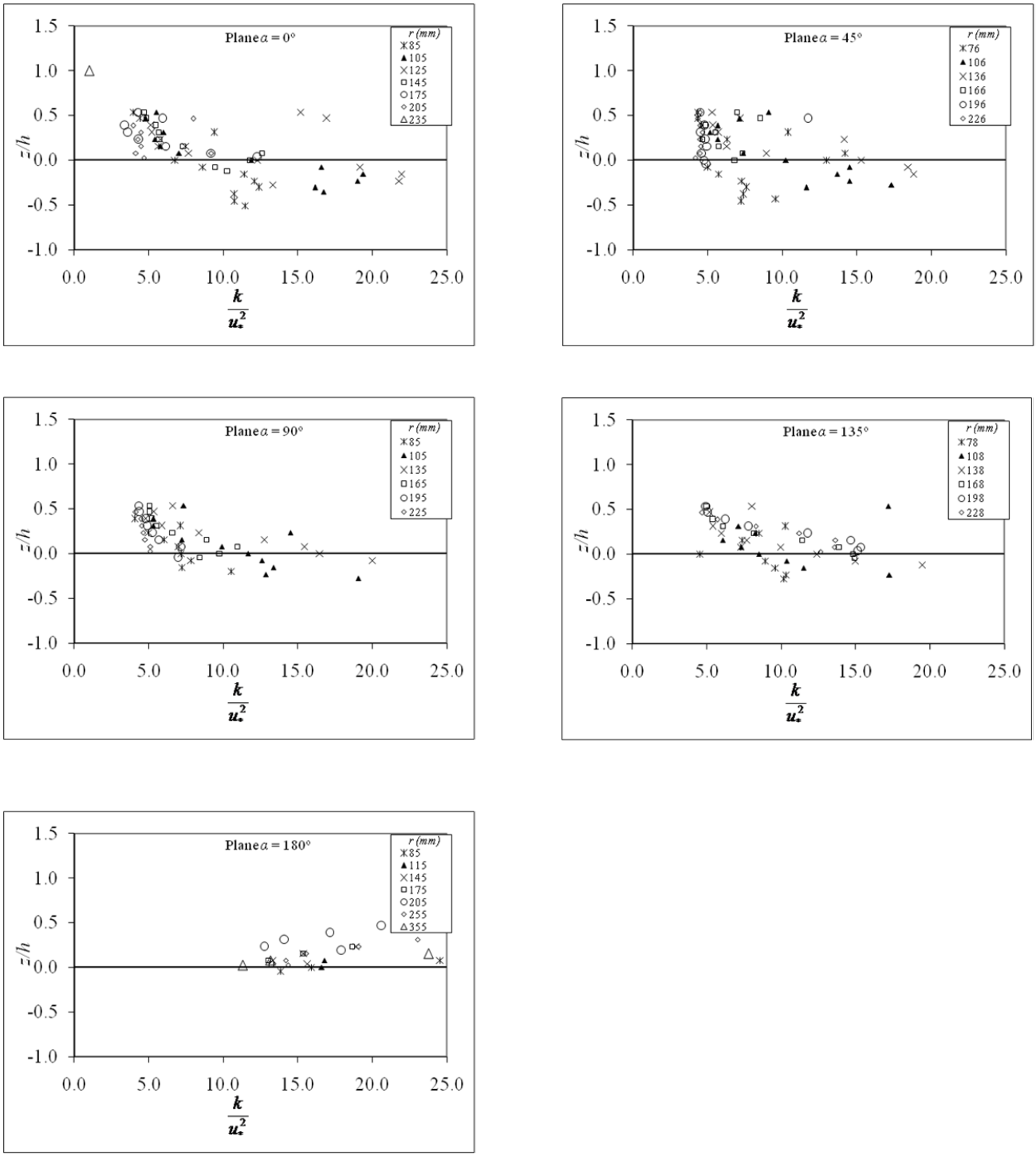

FIG. 4.3: Normalized profiles of turbulent kinetic energy measured around the circular uniform pier (*UPSH*) in different planes

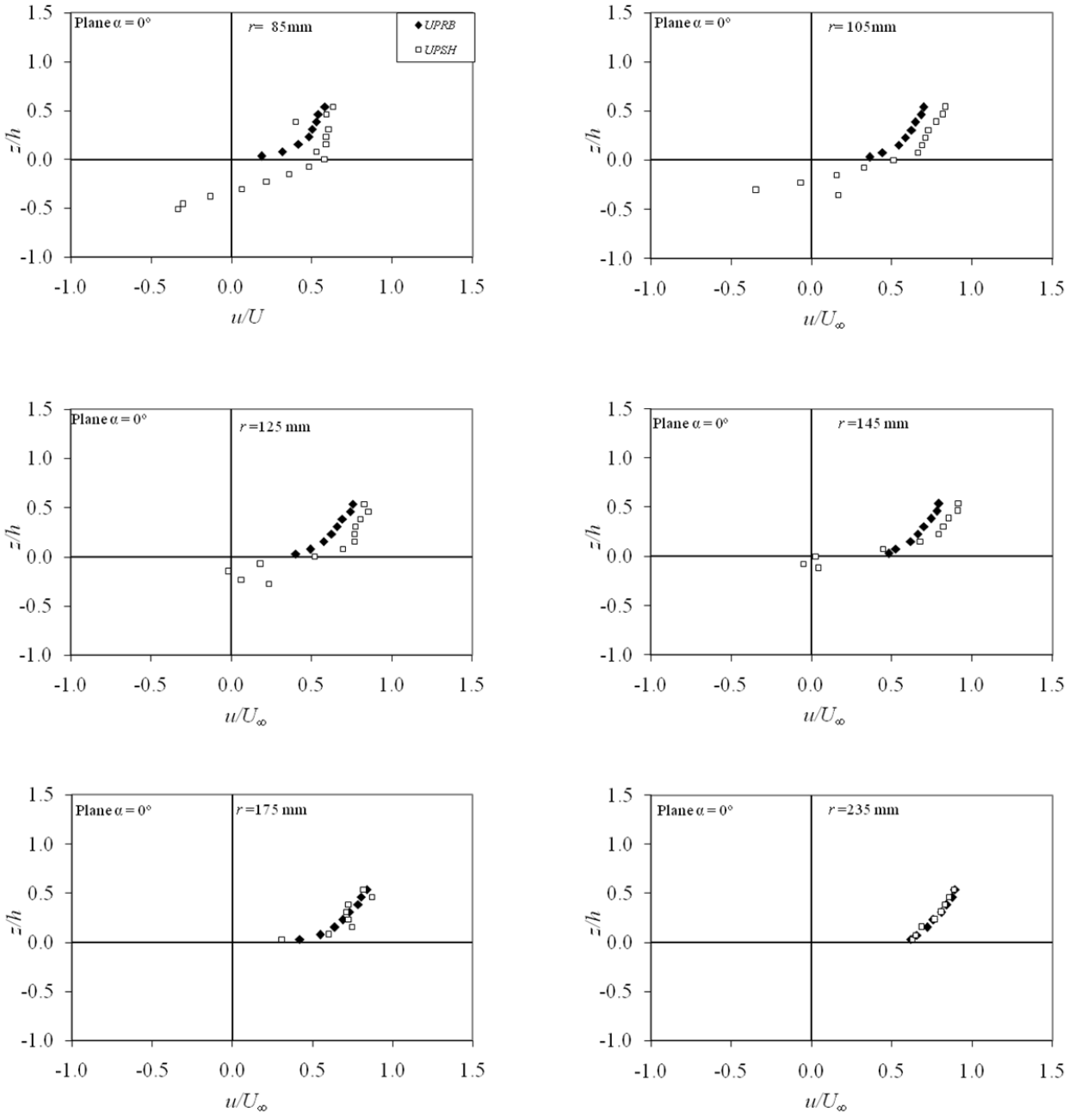

FIG. 4.4 (a): Comparison of normalized *u* component of velocity of circular uniform pier run (*UPRB*) with the circular compound pier run (*UPSH*) at plane α = 0º

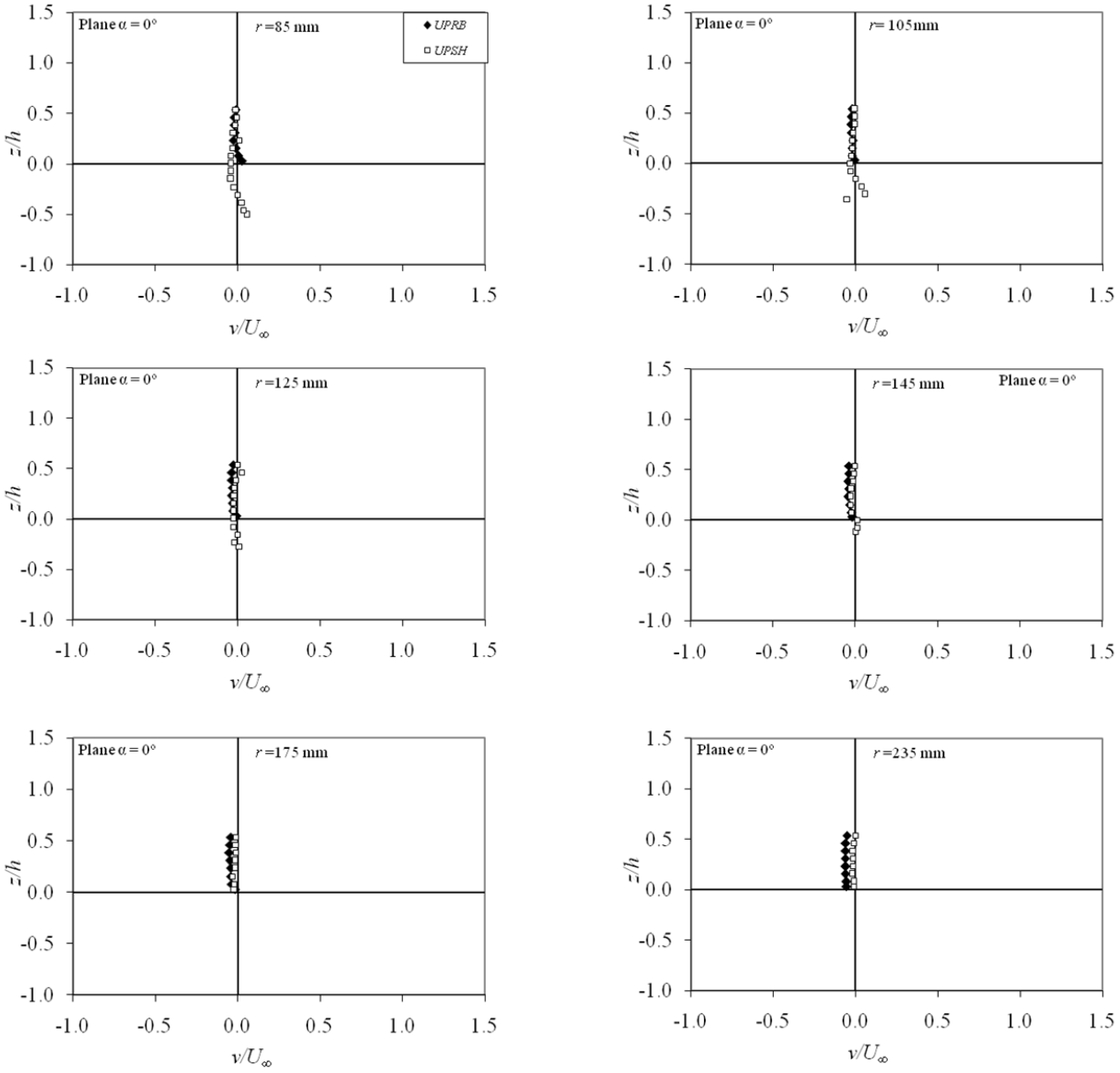

FIG. 4.4 (b): Comparison of normalized *v* component of velocity of circular uniform pier run (*UPRB*) with the circular compound pier run (*UPSH*) at plane α = 0º

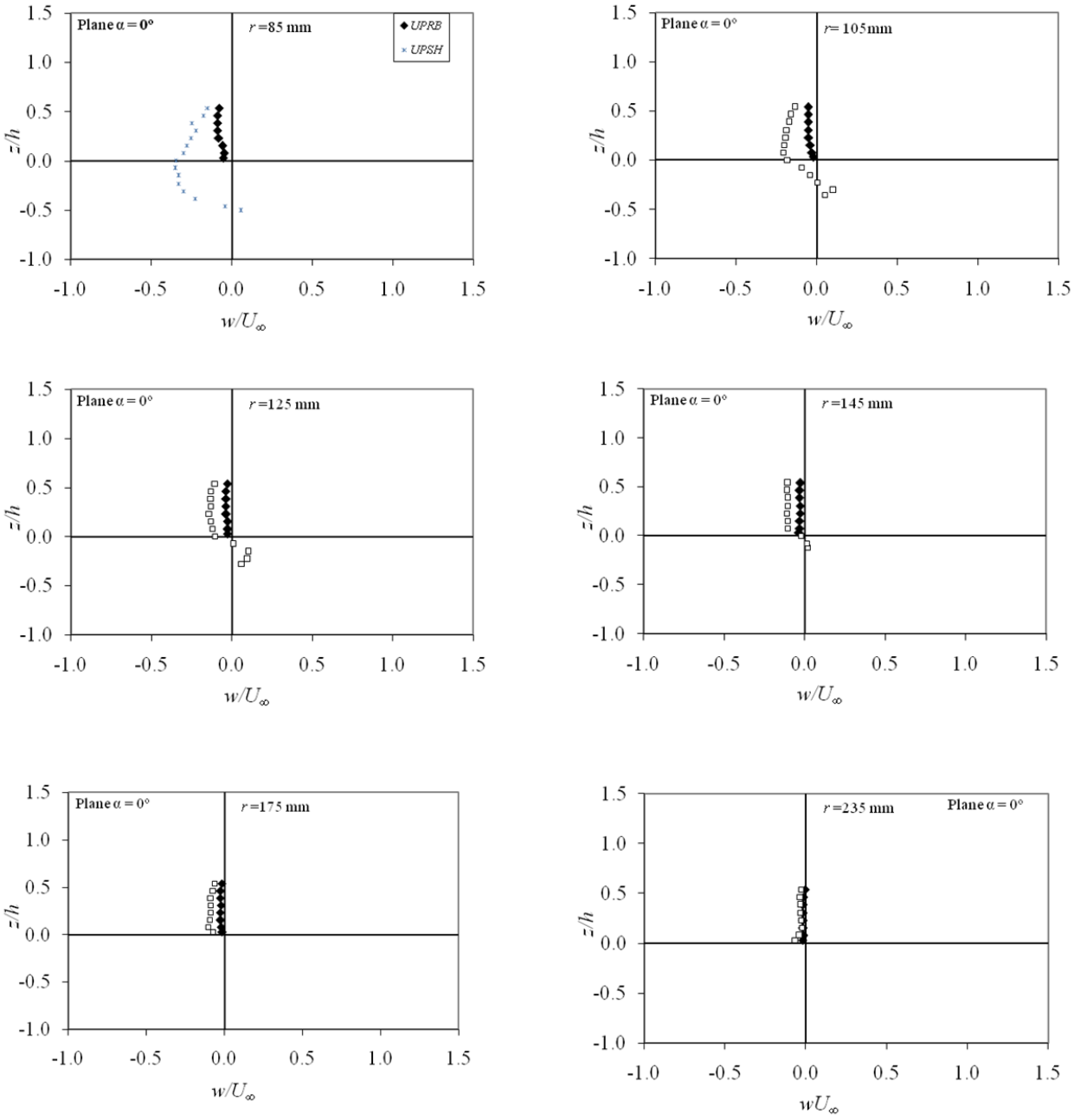

FIG. 4.4 (c): Comparison of normalized *w* component of velocity of circular uniform pier run (*UPRB*) with the circular compound pier run (*UPSH*) at plane α = 0º

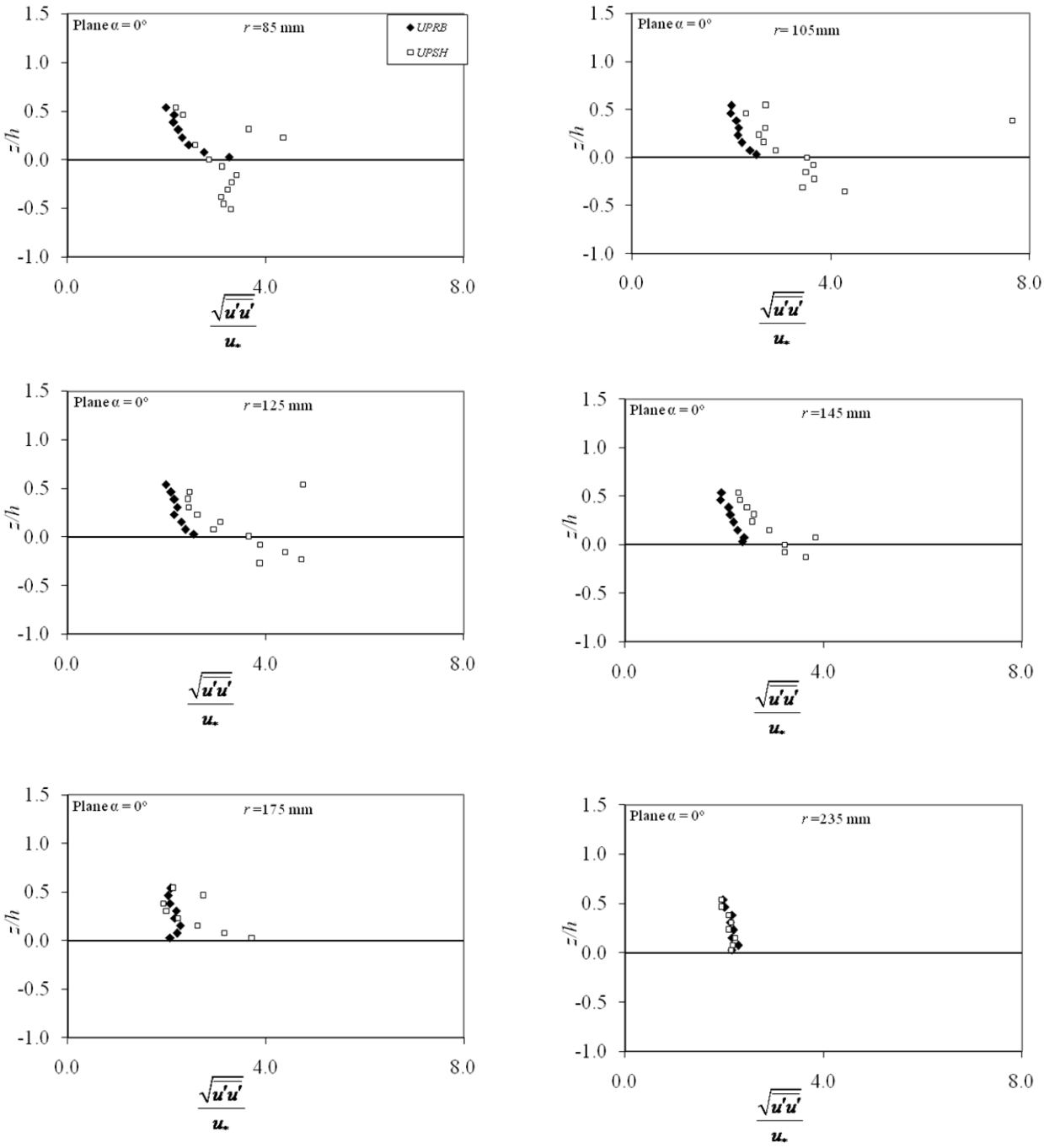

FIG. 4.5 (a): Comparison of normalized $\sqrt{u'u'}$ component of turbulence intensity of circular uniform pier run (*UPRB*) with the circular compound pier run (*UPSH*) at plane α = 0º

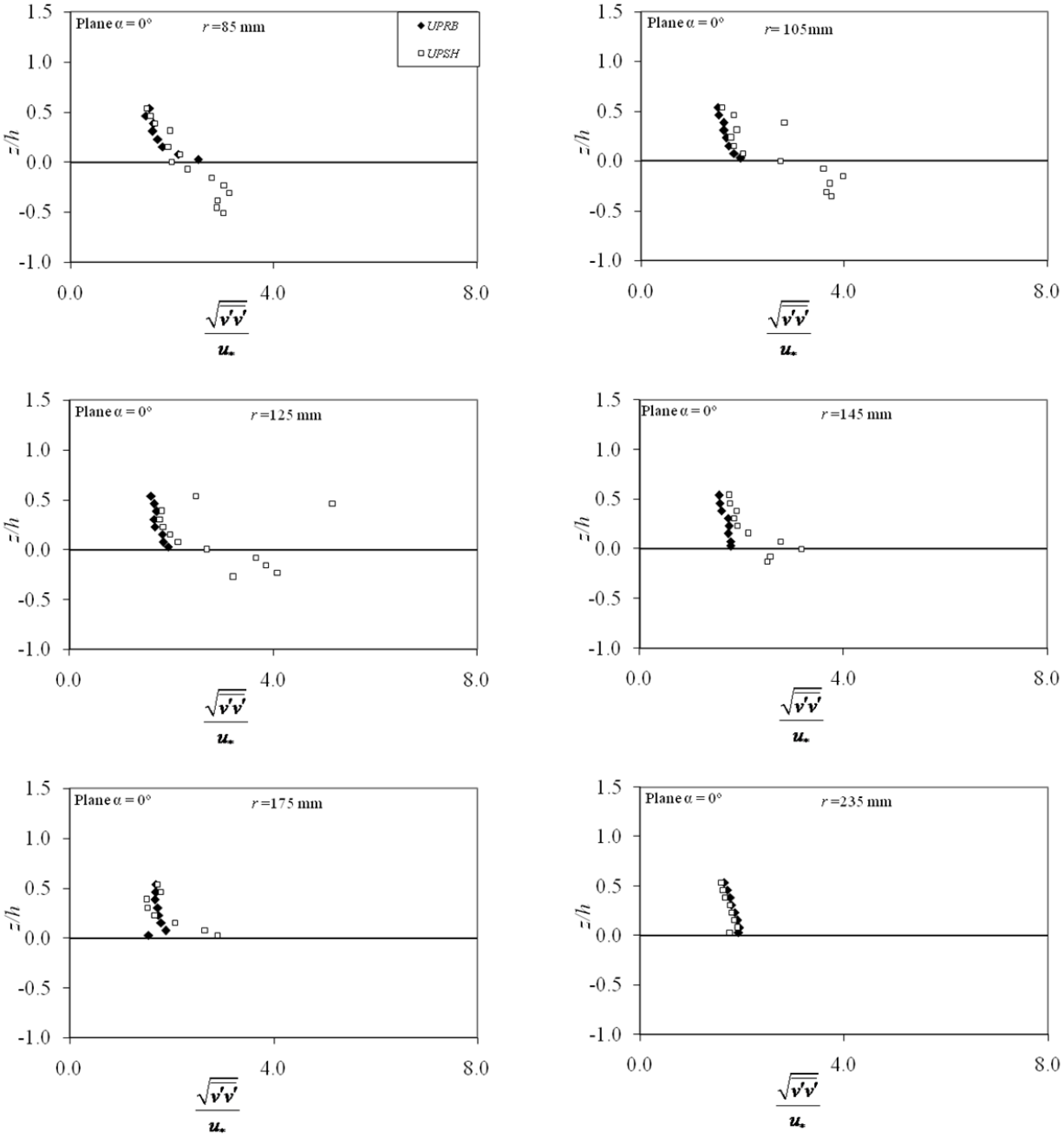

FIG. 4.5 (b): Comparison of normalized $\sqrt{\overline{v'v'}}$ component of turbulence intensity of circular uniform pier run (*UPRB*) with the circular compound pier run (*UPSH*) at plane α = 0º

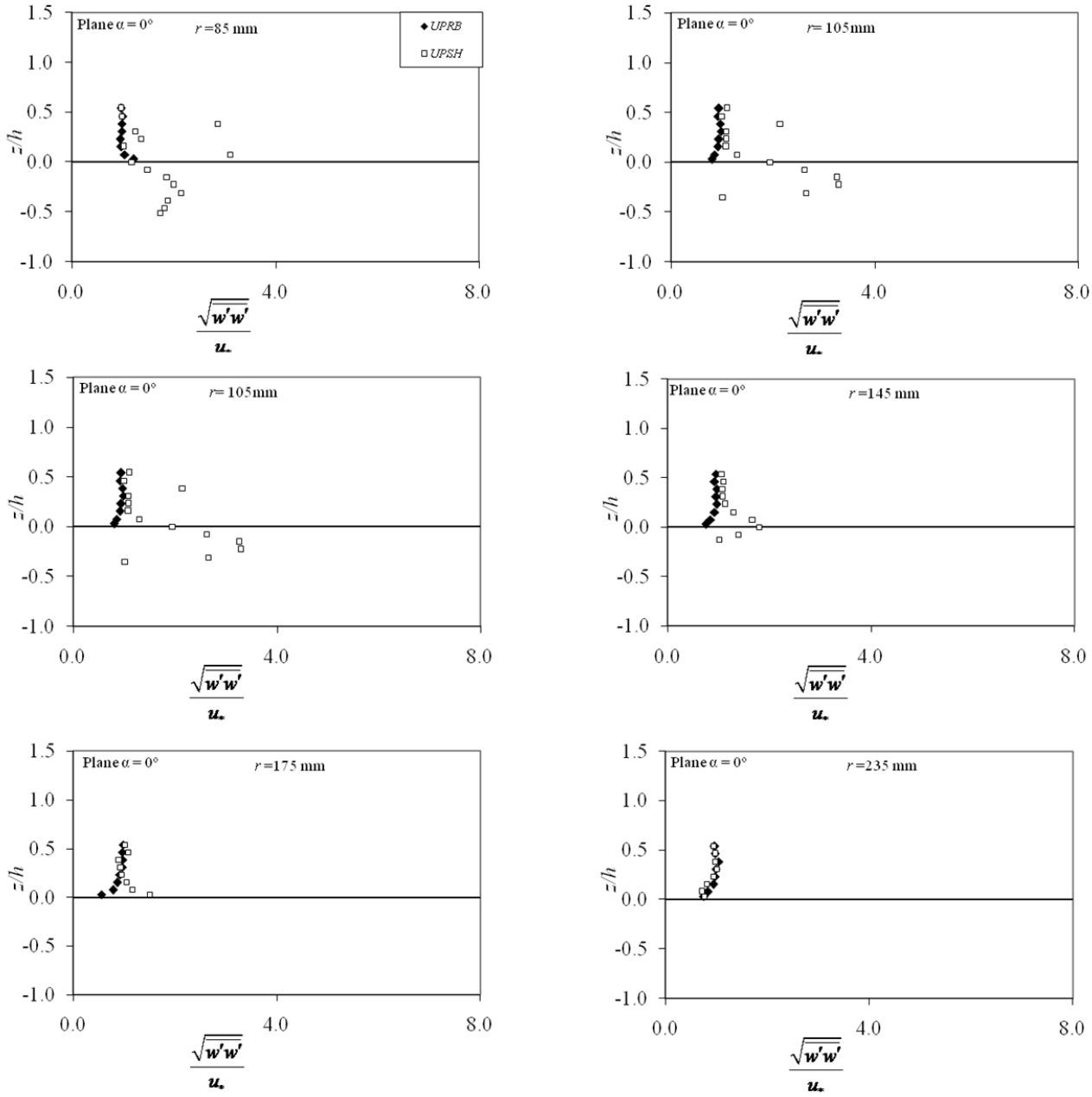

FIG. 4.5 (c): Comparison of normalized $\sqrt{\overline{w'w'}}$ component of turbulence intensity of circular uniform pier run (*UPRB*) with the circular compound pier run (*UPSH*) at plane α=0º

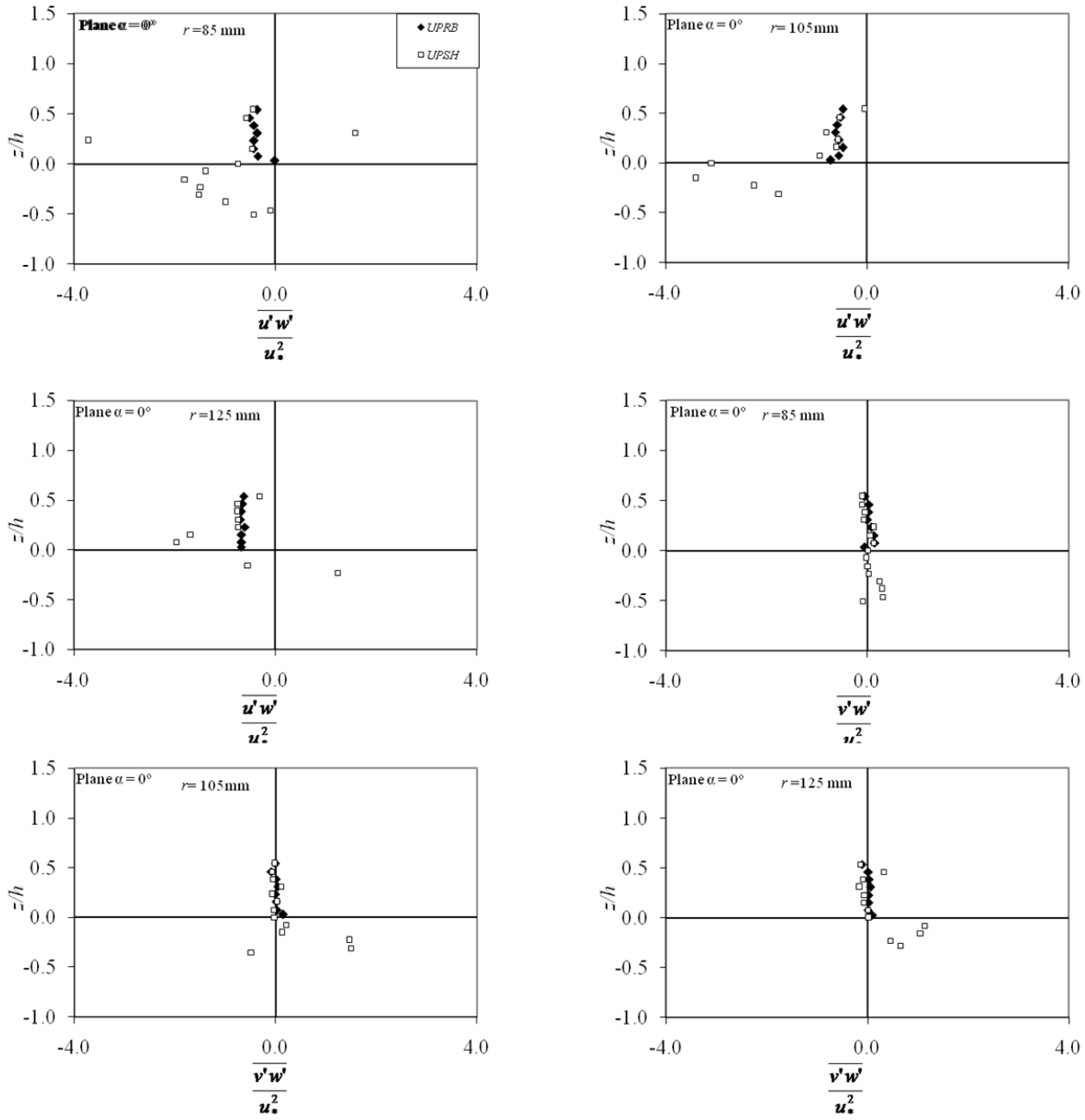

FIG. 4.5 (d): Comparison of normalized $\overline{u'w'}$ and $\overline{v'w'}$ component of Reynolds' stress of circular uniform pier run (*UPRB*) with the circular compound pier run (*UPSH*) at plane α = 0º

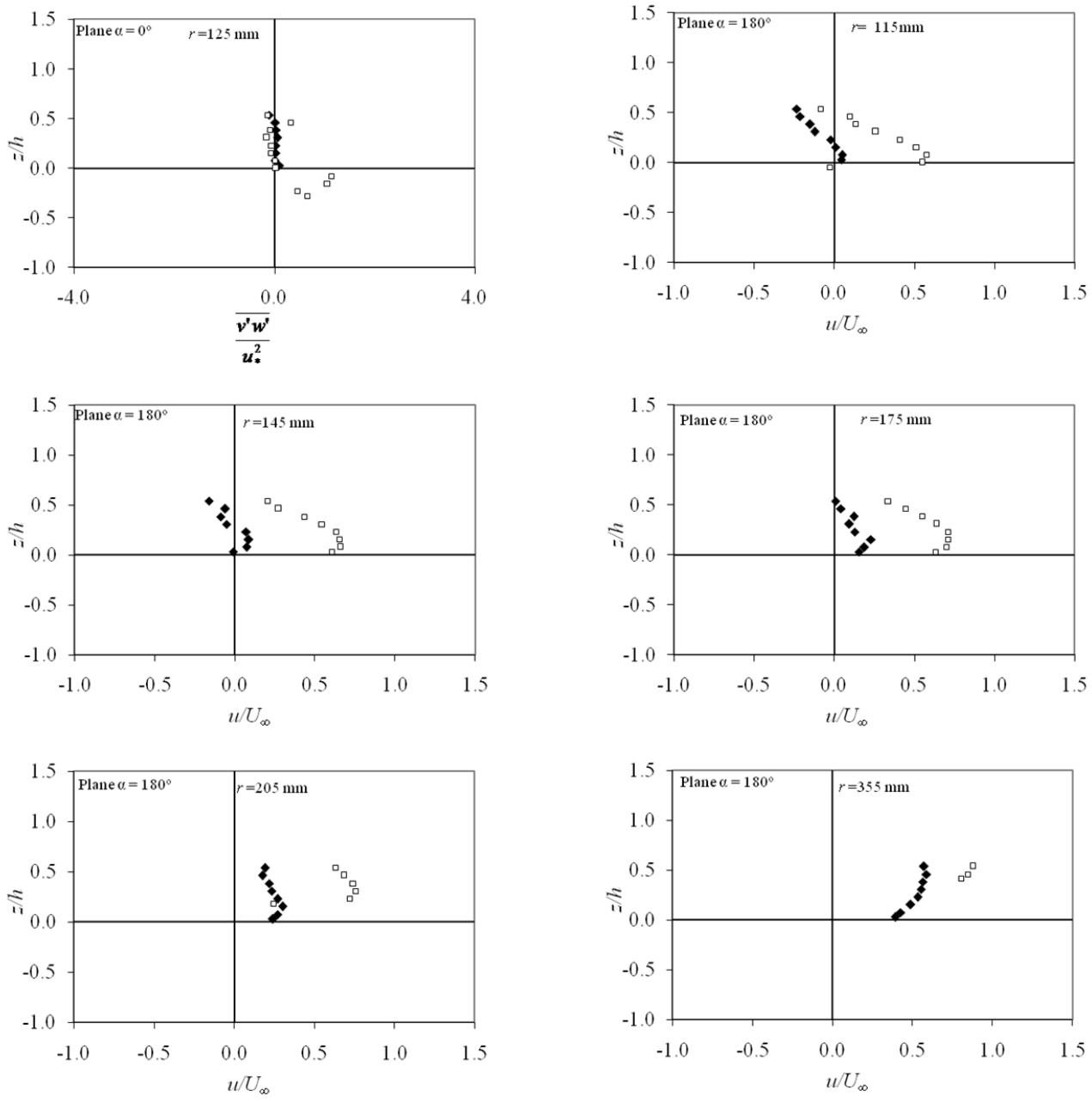

FIG. 4.6 (a): Comparison of normalized *u* component of velocity of circular uniform pier run (*UPRB*) with the circular compound pier run (*UPSH*) at plane α = 180º

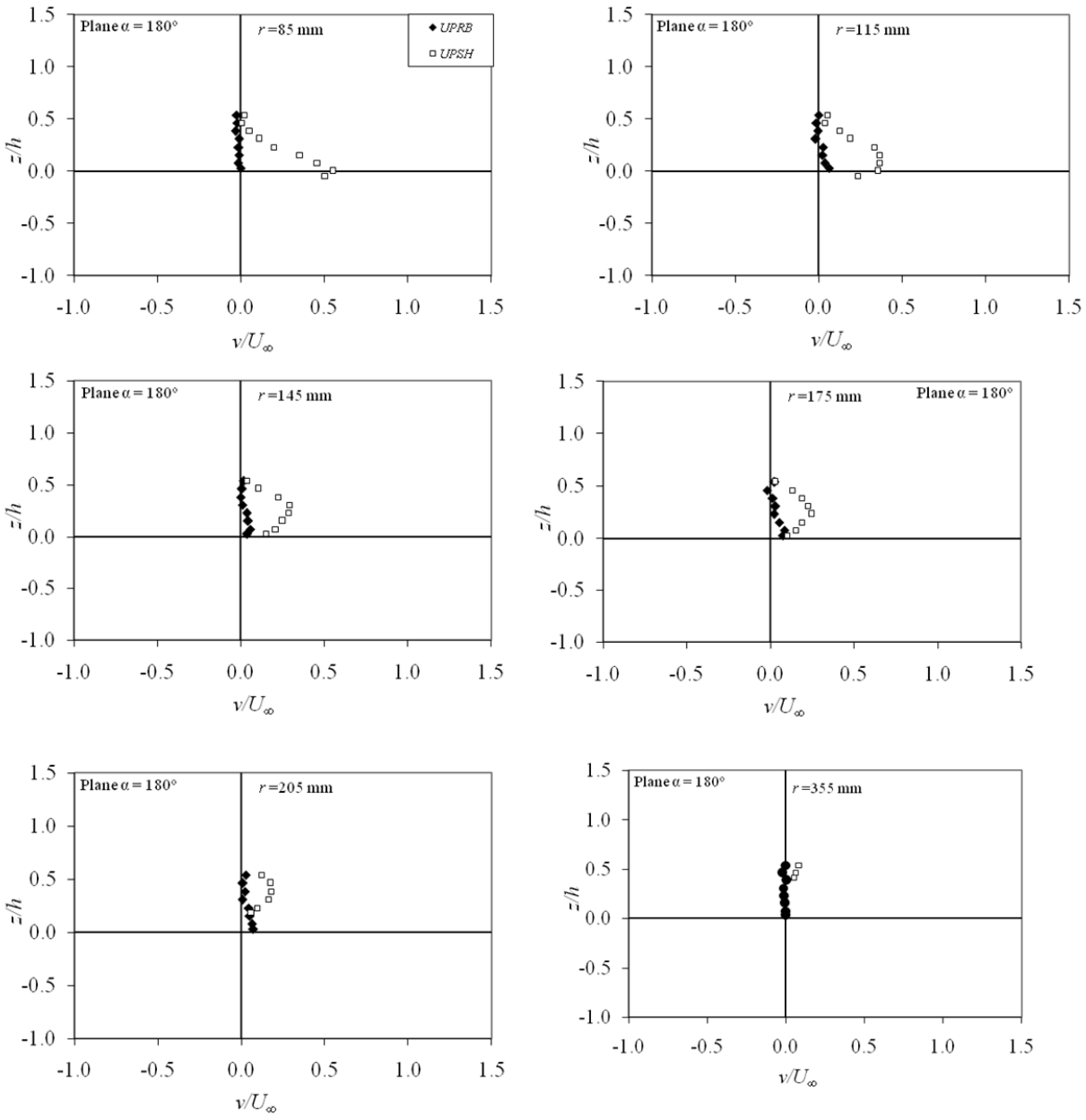

FIG. 4.6 (b): Comparison of normalized *v* component of velocity of circular uniform pier run (*UPSH*) with the circular compound pier run (*UPSH*) at plane α = 180º

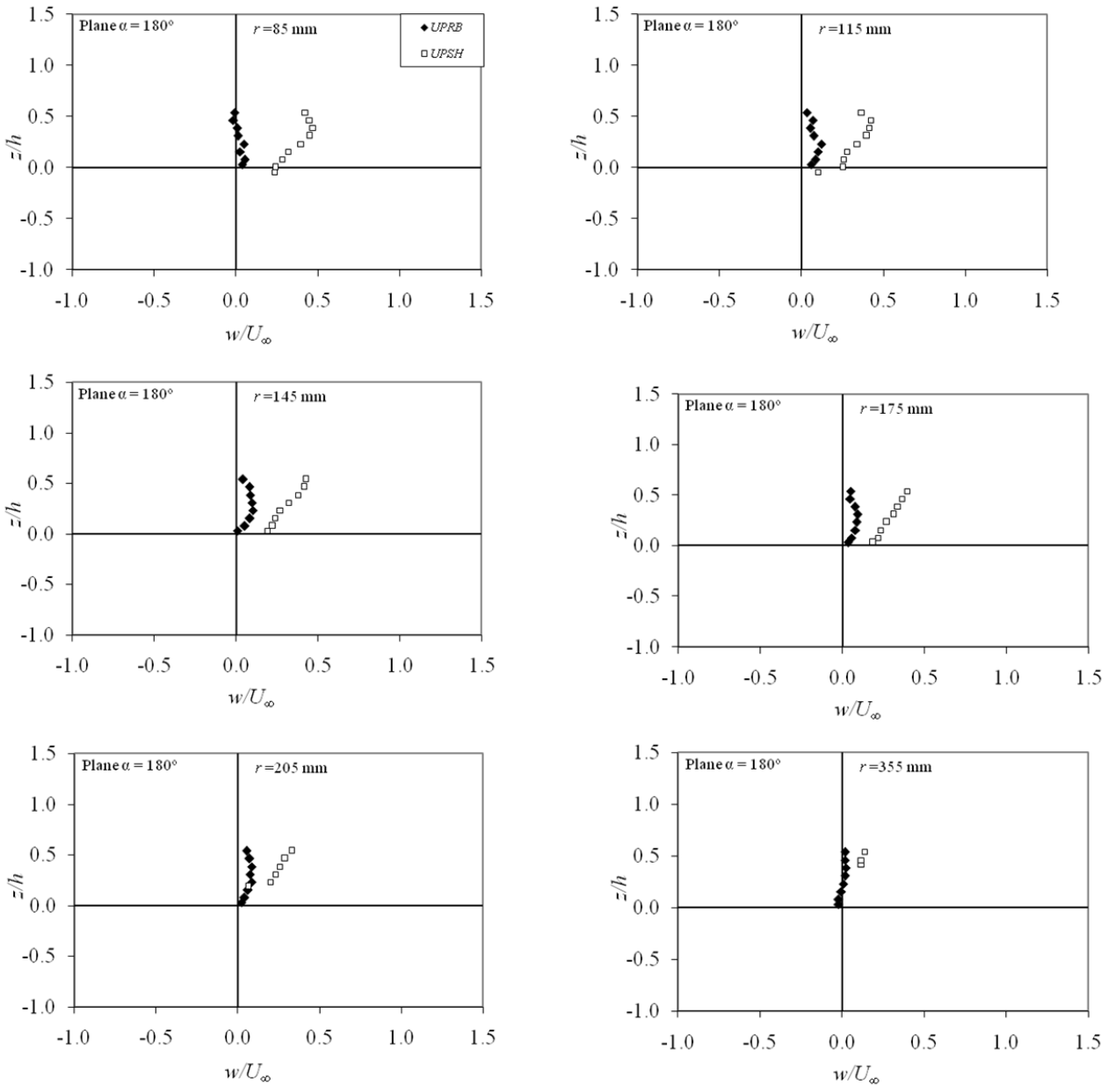

FIG. 4.6 (c): Comparison of normalized *w* component of velocity of circular uniform pier run (*UPRB*) with the circular compound pier run (*UPSH*) at plane α = 180º

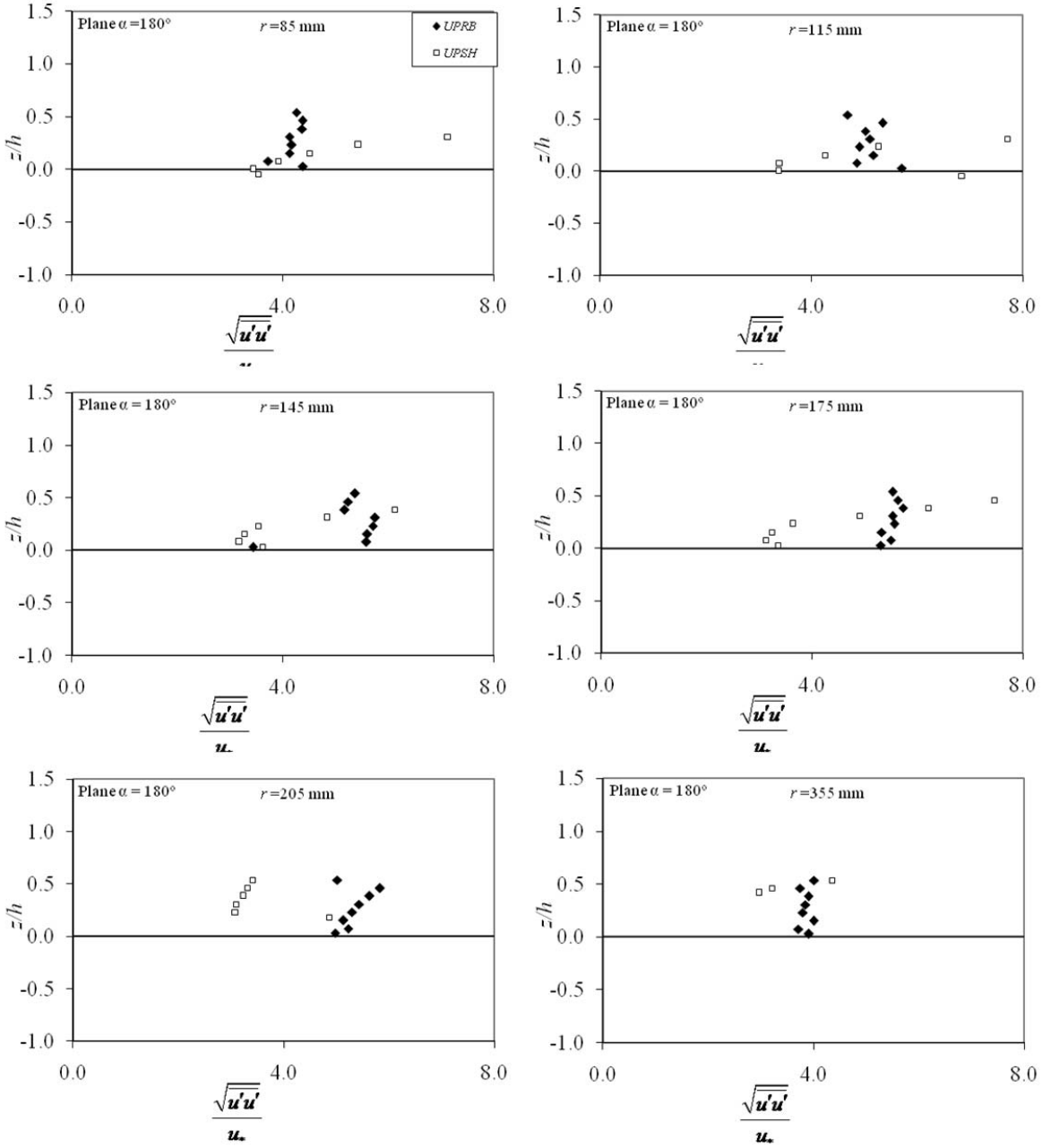

FIG. 4.7 (a): Comparison of normalized $\sqrt{\overline{u'u'}}$ component of turbulence intensity of circular uniform pier run (*UPRB*) with the circular compound pier run (*UPSH*) at plane α = 180º

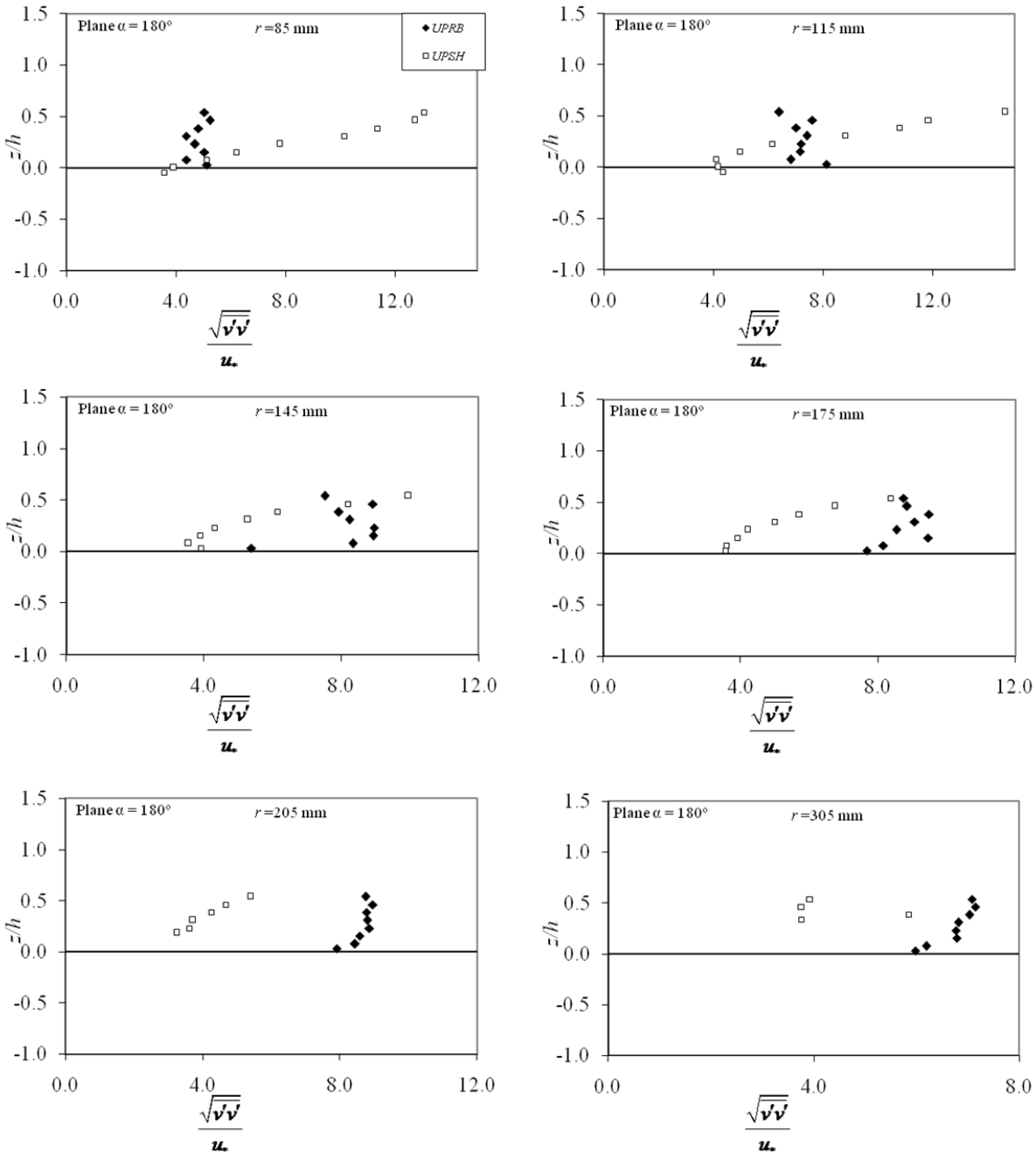

FIG. 4.7 (b): Comparison of normalized $\sqrt{\overline{v'v'}}$ component of turbulence intensity of circular uniform pier run (*UPRB*) with the circular compound pier run (*UPSH*) at plane α = 180º

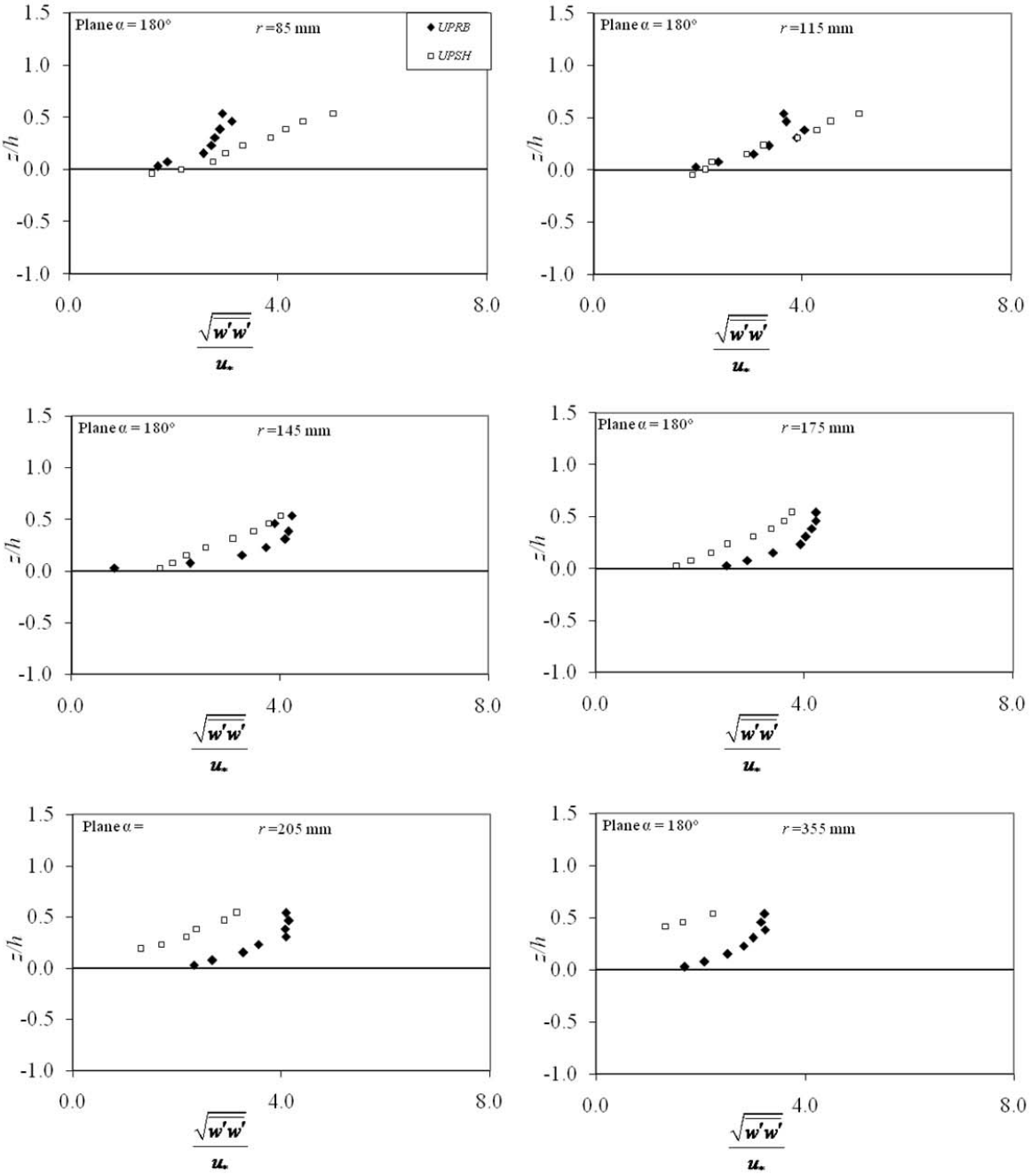

FIG. 4.7 (c): Comparison of normalized $\sqrt{w'w'}$ component of turbulence intensity of circular uniform pier run (*UPRB*) with the circular compound pier run (*UPSH*) at plane α = 180º

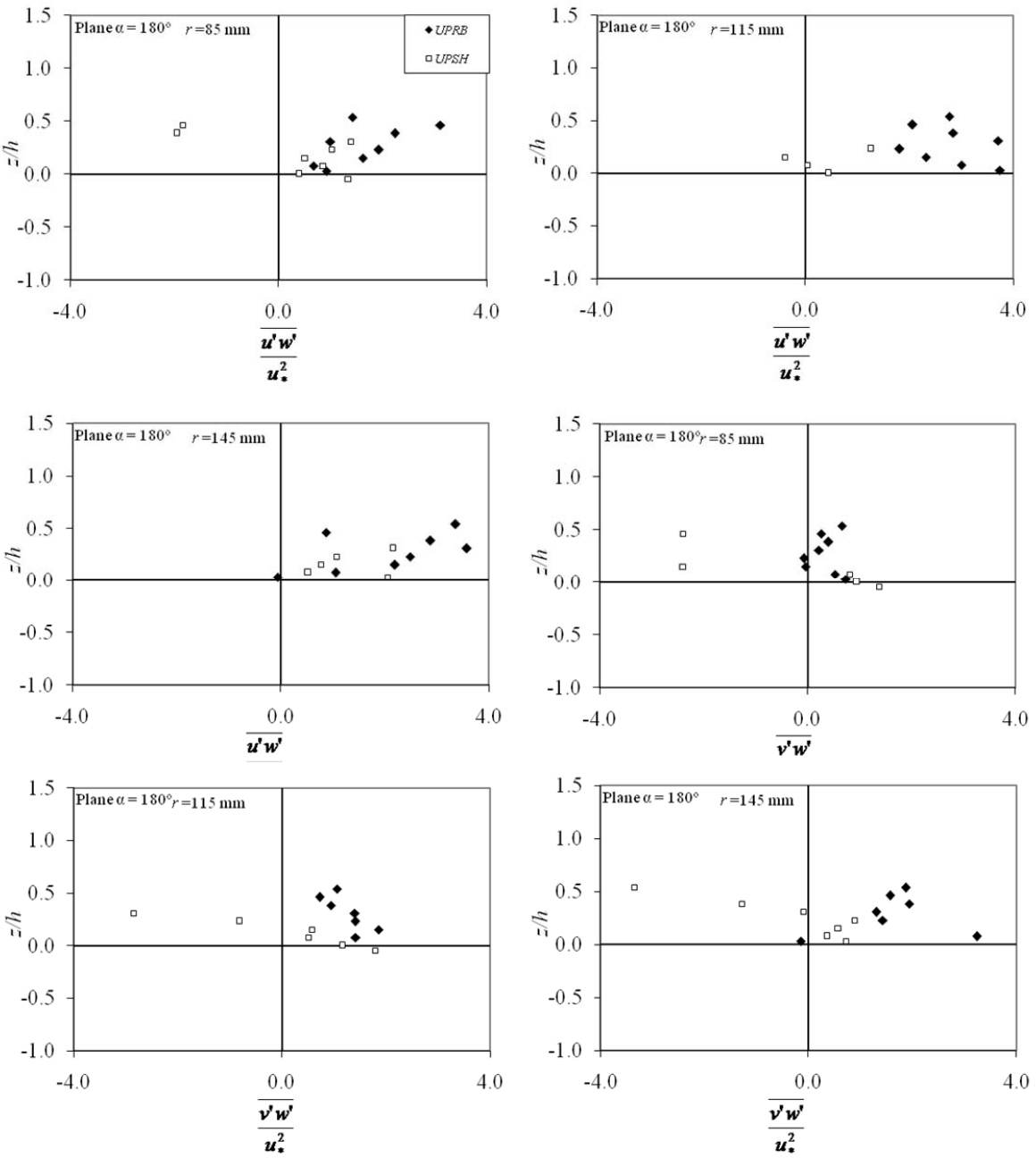

FIG. 4.7 (d): Comparison of normalized $\overline{u'w'}$ and $\overline{v'w'}$ component of Reynolds' stress of circular uniform pier run (*UPRB*) with the circular compound pier run (*UPSH*) at plane α = 180º

PLATE 4.1: Photographic view of the experimental flume

PLATE 4.3: Acoustic Doppler Velocimeter (*ADV*)

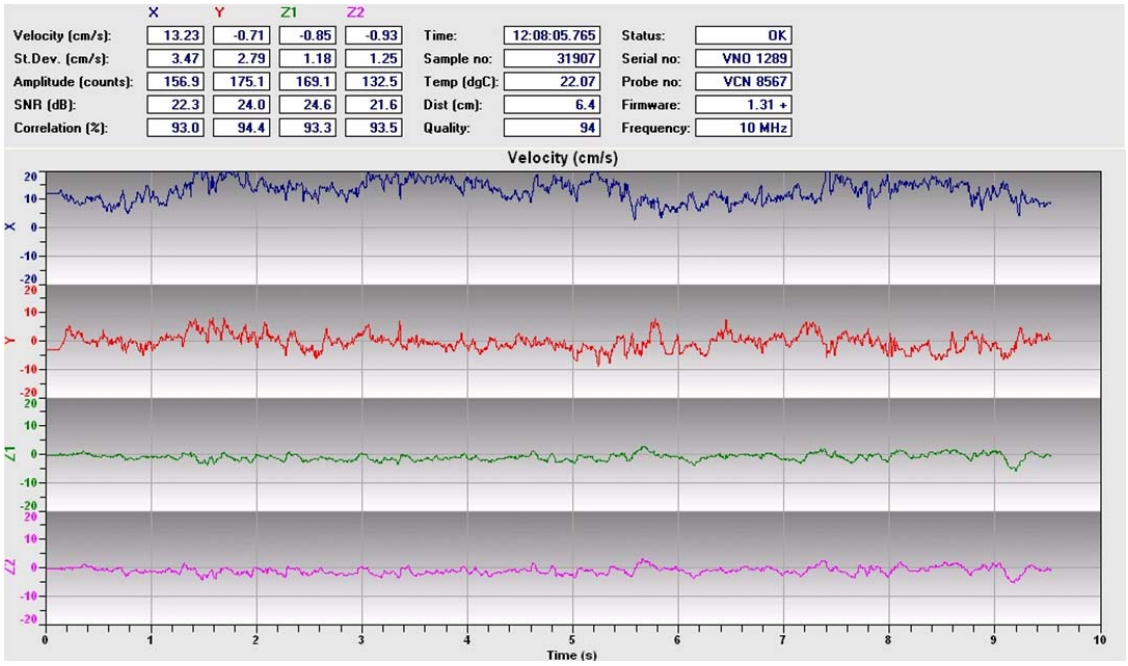

Screenshot taken at r = 10.5 cm 45 degrees with scour hole

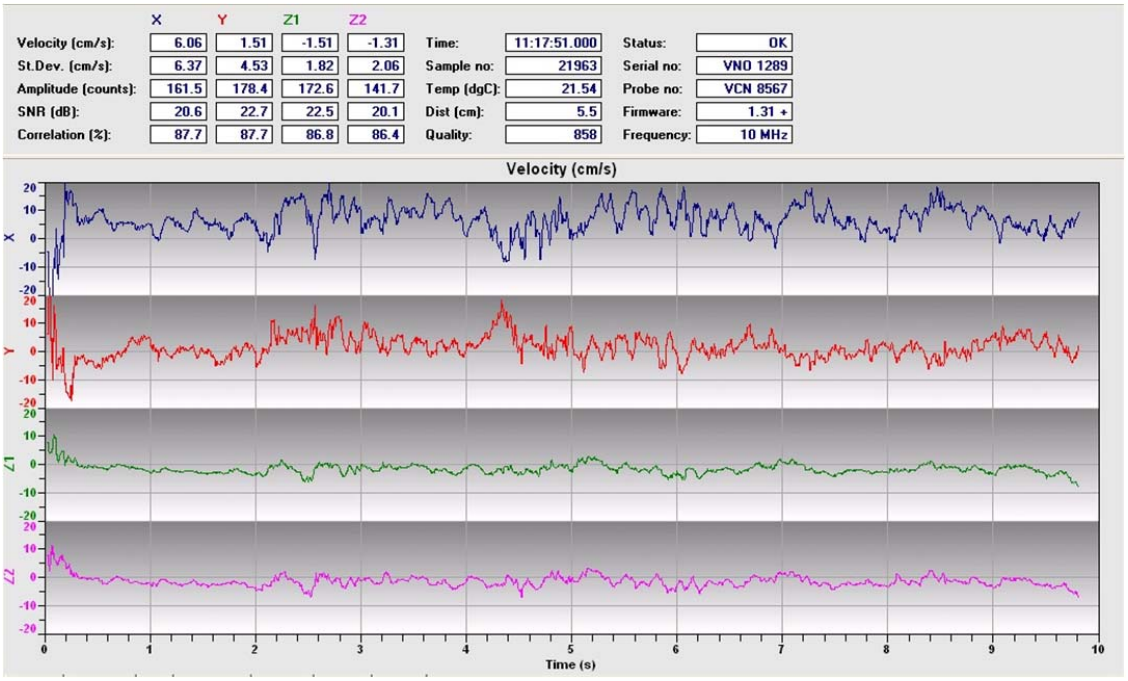

Screenshot taken at r = 85 cm 180 degrees without scour hole